ELSEVIER

Journal of Autoimmunity 30 (2008) 121–127

journal of autoimmunity

www.elsevier.com/locate/jautimm

Review

Cell and gene therapy using mesenchymal stem cells (MSCs)

Keiya Ozawa [a,b,*], Kazuya Sato [a], Iekuni Oh [a], Katsutoshi Ozaki [a], Ryosuke Uchibori [b], Yoko Obara [a,b], Yuji Kikuchi [a,b], Takayuki Ito [b], Takashi Okada [b,1], Masashi Urabe [b], Hiroaki Mizukami [b], Akihiro Kume [b]

[a] *Division of Hematology, Department of Medicine, Jichi Medical University, 3311-1 Yakushiji, Shimotsuke-shi, Tochigi 329-0498, Japan*
[b] *Division of Genetic Therapeutics, Center for Molecular Medicine, Jichi Medical University, 3311-1 Yakushiji, Shimotsuke-shi, Tochigi 329-0498, Japan*

Abstract

Mesenchymal stem cells (MSCs) are considered to be a promising platform for cell and gene therapy for a variety of diseases. First, in the field of hematopoietic stem cell transplantation, there are two applications of MSCs: 1) the improvement of stem cell engrafting and the acceleration of hematopoietic reconstitution based on the hematopoiesis-supporting ability; and 2) the treatment of severe graft-versus-host disease (GVHD) based on the immunomodulatory ability. Regarding the immunosuppressive ability, we found that nitric oxide (NO) is involved in the MSC-mediated suppression of T cell proliferation. Second, tumor-bearing nude mice were injected with luciferase-expressing MSCs. An in vivo imaging analysis showed the significant accumulation of the MSCs at the site of tumors. The findings suggest that MSCs can be utilized to target metastatic tumors and to deliver anti-cancer molecules locally. As the third application, MSCs may be utilized as a cellular vehicle for protein-supplement gene therapy. When long-term transgene expression is needed, a therapeutic gene should be introduced with a minimal risk of insertional mutagenesis. To this end, site-specific integration into the AAVS1 locus on the chromosome 19 (19q13.4) by using the integration machinery of adeno-associated virus (AAV) would be particularly valuable. There will be wide-ranging applications of MSCs to frontier medical treatments in the near future.

Keywords: Cancer gene therapy; GVHD; Mesenchymal stem cells; Site-specific integration; Tumor targeting

1. Introduction

In bone marrow, there are different types of tissue stem cells (adult stem cells); i.e. hematopoietic stem cells and mesenchymal stem cells (MSCs). MSCs account for a small population of cells in bone marrow as a non-hematopoietic component with the capacity to differentiate into a variety of cell lineages, including adipocytes, osteocytes, chondrocytes, muscles, and stromal cells [1]. Recent studies demonstrated that MSCs are capable of supporting hematopoiesis and of regulating immune response [2]. In addition, since MSCs can be readily isolated and expanded *in vitro*, they are expected to be a source of cell therapy. Interestingly, MSCs have the ability to accumulate at the site of: i) tissue/organ damage; ii) inflammation; and iii) cancer when administered *in vivo*. Therefore, MSCs can be utilized for: i) regenerative therapy; ii) treatment of graft-versus-host disease (GVHD) and Crohn disease; and iii) platform of cancer gene therapy (targeted delivery of anti-cancer agents). Another unique feature of MSCs is little or low immunogenicity due to the lack of expression of co-stimulatory molecules. This phenomenon makes it possible to administer MSCs without HLA matching for cell therapy. A single lot of expanded MSCs from one healthy donor can be utilized for treatment of many patients. Although clinical applications of MSCs have been conducted for the suppression of severe acute GVHD in allogeneic stem cell transplantation [3,4] and for regenerative therapy [5,6], molecular mechanisms underlying the biological effects of

* Corresponding author. Jichi Medical University, Division of Hematology, Department of Medicine, 3311-1 Yakushiji, Shimotsuke-shi, Tochigi, 329-0498, Japan. Tel.: +81 285 58 7353; fax: +81 285 44 5258.
E-mail address: kozawa@ms2.jichi.ac.jp (K. Ozawa).
[1] Present address: Department of Molecular Therapy, National Institute of Neuroscience, National Center of Neurology and Psychiatry, 4-1-1 Ogawa-Higashi, Kodaira, Tokyo 187-8502, Japan.

0896-8411/$ - see front matter © 2008 Elsevier Ltd. All rights reserved.
doi:10.1016/j.jaut.2007.12.008

MSCs remains obscure. Finding key molecules for differentiation, immunosuppression, and hematopoietic support of MSCs would be valuable for further augmenting the efficacy of MSCs in a wide range of clinical applications. In this regard, development of the technology for genetic manipulation of MSCs is also important research project. Site-specific integration of a therapeutic gene into a safe locus in the genome should be investigated from the safety standpoint.

2. Microarray analysis of genes responsible for differentiation of mesenchymal stem cells

Genes regulating the differentiation of MSCs remain obscure and it is technically difficult to do high-throughput analysis using primary MSCs, because such cells contain heterogeneous populations. To overcome the problems related to the heterogeneity of primary MSCs, we utilized MSC-like cell lines. It has been shown that 10T1/2 cells, derived from C3H mouse embryo cells, differentiate into adipocytes, osteocytes, and chondrocytes with a treatment of 5-azacytidine. We previously established two sub-lines from 10T1/2, designated as A54 for a preadipocyte cell line and M1601 for a myoblast cell line [7]. Under appropriate culture conditions, A54 and M1601 cells terminally differentiate into adipocytes and myotubes, respectively, while parental 10T1/2 cells remain undifferentiated under the same culture conditions. Therefore, 10T1/2 cells can be utilized as a model of MSCs, and A54 and M1601 are used as committed mesenchymal progenitors. Gene expression profiles of these cell lines were compared by microarray analysis before and after differentiation.

Each of parent 10T1/2, A54, and M1601 cell lines showed a distinctive and unique gene expression profile despite morphological similarity (Fig. 1) [8]. Parental 10T1/2 cells had 105 elevated genes including ones encoding Activin, Dlk, Nov, Grb10, p15, and many functionally unknown molecules. Dlk and Nov are known to be involved in Notch signaling pathway and were reported to have the ability to inhibit differentiation into adipocytes and osteoblasts [9]. In preadipocyte A54 cells, 201 genes were up-regulated, including genes known to be involved in adipocyte differentiation such as genes encoding C/EBPα, C/EBPδ, PPAR-γ, PAI-I, and Frizzled-1 [10]. Myoblasts M1601 cells showed 137 up-regulated genes, including ones related to skeletal muscle differentiation such as genes encoding MyoD, MLC1F, α-skeletal actin, myosin heavy chain, and myosin light chain [11] as well as genes related to cardiac muscle differentiation such as genes encoding α-cardiac actin, cardiac troponin C, and troponin T2 [12].

Previous studies have shown that preadipocytes have a higher ability to support hematopoiesis than other kinds of stromal cell components *in vitro* [12,13]. Our results of gene expression profile revealed up-regulation of critical cytokines for hematopoiesis such as SCF and SDF-1 in preadipocyte A54 cells. In addition, many chemokines, such as CXCL-1 and CCL-7, were also up-regulated. Since Ang-1 was reported to be indispensable for the self-renewal of hematopoietic stem cells [14], we performed real-time PCR analysis of Ang-1 along with SCF, SDF-1, CEBP-δ, IGF-1, and CXCL-1. The expression of these genes was highest in A54 cells among the three cell lines. Moreover, protein expression of Ang-1 was only detected in A54 among three cell lines and the level of this protein decreased after adipocyte differentiation.

To examine the effects of these three lines on hematopoiesis, we co-cultured mouse hematopoietic stem cell fraction with these three stromal cell lines. The cells in Lin(−)Sca-1(+) fraction were plated on 10T1/2, A54, or M1601 cells.

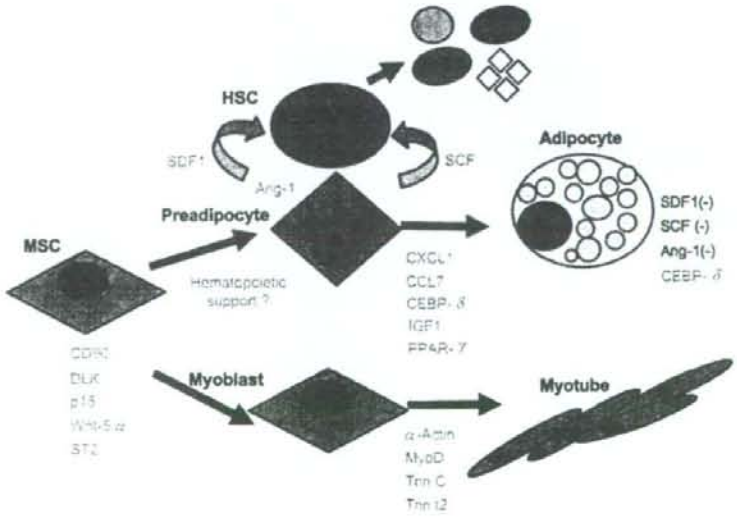

Fig. 1. Proposed model for the hierarchy of the bone marrow stromal system [8].

After 6 days of co-culture, hematopoietic progenitors were detected only on the A54 cells. These results suggest that only A54 cells have the ability to support hematopoietic cell growth among these three cell lines, consistent with the previous report. Hematopoietic cell proliferation was not observed on the layer of the terminally differentiated A54 adipocytes, suggesting that A54 cells lose the ability for hematopoietic cell support after adipocyte differentiation. To understand the molecular mechanisms of this observation, we examined the expression levels of SCF, SDF-1, and Ang-1 during adipocyte differentiation by RT real-time PCR. The expression levels of Ang-1 and SCF decreased immediately after the induction of adipocyte differentiation, and that of SDF-1 decreased gradually. In contrast to this, the level of adipocyte differentiation marker, CEBP-δ, was unchanged.

The analysis of functionally unknown molecules is currently underway. In addition, cell-to-cell contact is also believed to be crucial in the interaction between hematopoietic stem cells and MSCs. We are currently investigating the cellular and molecular events in the interactive communication between hematopoietic stem cells and MSCs.

3. Nitric oxide (NO) plays a critical role in suppression of T-cell proliferation by mesenchymal stem cells

There is a case report of severe steroid-resistant GVHD after bone marrow transplantation, in which intravenous infusion of MSCs greatly improved clinical manifestations [3]. Moreover, multi-institutional clinical trial of MSC-treatment of severe grade III–IV acute GVHD in Europe revealed very high overall response rate (about 70%) (Le Blanc et al., ASH meeting 2006). The molecular mechanisms by which MSCs suppress T-cell proliferation are complicated, and whether a soluble factor plays a major role remains controversial. Transforming growth factor-β (TGF-β), hepatocyte growth factor (HGF), indoleamine 2,3-dioxygenase (IDO), and prostaglandin E_2 (PGE_2) have been reported to mediate T-cell suppression by MSCs [15–17]. In addition, some reports have shown that a soluble factor is the major mediator of suppression, whereas some reports have demonstrated that T-cell-MSC contact is required for this suppression.

We also investigated the molecular mechanisms using primary murine MSCs, and focused on nitric oxide (NO), because it is known to inhibit T-cell proliferation. NO is produced by NO synthases (NOSs), of which there are 3 subtypes; i.e. inducible NOS (iNOS), endothelial NOS, and neuronal NOS. It has been known that macrophages suppress T-cell proliferation, and that this suppression is caused by NO-mediated inhibition of Stat5 phosphorylation [18]. We investigated whether MSCs can also produce NO and whether NO is involved in their ability to suppress T-cell proliferation [19].

T cells proliferated in response to PMA and ionomycin, which act downstream of the T-cell-receptor complex by activating protein kinase C and inducing Ca^{2+} influx, respectively. Such T-cell proliferation was suppressed by the presence of MSC, suggesting that MSCs influence signals downstream of protein kinase C and Ca^{2+} influx. The expression of the activation markers CD25 and CD69 on CD4 or CD8 T cells did not change even in the presence of MSCs. MSCs suppressed the production of IFN-γ but not IL-2.

Although T cells from $Stat5^{-/-}$ mice do not proliferate upon stimulation with anti-CD3, they up-regulate CD25. Because this phenotype is similar to the status of activated T cells in the presence of MSCs, we hypothesized that MSCs suppress Stat5 phosphorylation. Indeed, Stat5 phosphorylation in activated T cells was diminished in the presence of MSCs. We found that MSCs caused a significant and cell-dose-dependent production of NO only when co-cultured with activated T cells. The induction of iNOS was readily detected in MSCs but not in T cells. RT-PCR and Western blot analysis detected iNOS expression in MSCs cocultured with activated splenocytes but not in MSCs or splenocytes when cultured alone. The immunofluorescence studies showed that iNOS was exclusively expressed in $CD45^-$ adherent cells, which correspond to MSCs, but not in $CD45^+$T cells. Next, we investigated the effects of *N*-nitro-L-arginine methyl ester (L-NAME), a specific inhibitor of NOS. As expected, L-NAME dose-dependently inhibited the production of NO by MSCs in the presence of activated T cells. Importantly, L-NAME restored T-cell proliferation and Stat5 phosphorylation, indicating that NO is involved in the inhibition of T-cell proliferation and Stat5 phosphorylation. Moreover, MSCs from inducible $NOS^{-/-}$ mice had a reduced ability to suppress T-cell proliferation.

In the presence of direct interaction between T cells and MSCs, there was a high level of NO production accompanied by a strong suppression of T-cell proliferation. In contrast, both NO production and T-cell suppression were reduced in a transwell system, in which T cells were separated from MSCs by a 1-μm-pore membrane. There are two possible explanations for the difference in T-cell suppression between the presence and absence of the transwell system. First, the amount of NO produced in the transwell system was lower than that in the presence of direct interaction. This finding suggests that direct interaction is critical for efficient production of NO as well as for strong suppression of T-cell proliferation. A second possible explanation is that, because NO is highly unstable, it can lose its activity before it reaches T cells in the transwell system.

Because TGF-β, IDO, and PGE_2 were reported as mediators of T-cell suppression by MSCs, we compared the effects of L-NAME with inhibitors of each mediator. Indomethacin (inhibitor of PGE_2 production) but not 1-methyl-DL-tryptophan (1-MT: inhibitor of IDO) or an anti-TGF-β-neutralizing antibody restored T-cell proliferation as effectively as L-NAME; however, the effects of L-NAME and indomethacin were not additive, suggesting that the NO and PGE_2 share signaling pathways leading to T-cell suppression.

In summary, our hypothesis that NO is produced by MSCs and that it suppresses T-cell proliferation in part through inhibition of Stat5 phosphorylation was supported by the following facts: (1) NO was readily detected in the medium in the co-culture of MSCs and activated T cells; (2) L-NAME restored T-cell proliferation as well as Stat5 phosphorylation; and (3) MSCs from $iNOS^{-/-}$ mice had markedly

reduced ability to suppress T-cell proliferation. This hypothesis was further confirmed by the finding that iNOS expression was detected only in MSCs co-cultured with activated T cells.

In our scenario (Fig. 2), when MSCs are administered to the patients with severe acute GVHD, MSCs are considered to accumulate at the site of inflammation. Upon interaction with activated T cells, MSCs express iNOS and produce NO, which suppresses T-cell proliferation via inhibition of STAT5 phosphorylation. Systemic adverse effects of NO do not occur due to local production of NO with very short half-life. This is a very important point, because conventional treatment of acute GVHD causes severe systemic immunosuppression, which sometimes leads to life-threatening infections. Since MSC treatment causes just local immunosuppression, it should be much safer.

4. Interferon-γ and NF-κB mediate nitric oxide production by mesenchymal stem cells

Human MSCs were reported to suppress Th1 differentiation and augment Th2 differentiation. Therefore, we investigated whether mouse bone-marrow-derived MSCs and the 10T1/2 cell lines have the same effect on Th1 and Th2. We found a reverse correlation between NO production and T cell proliferation in Th1/Th2 conditions, where NO production was highly induced in the presence of MSCs in Th1 but it was only minimally induced in Th2. In particular, primary MSCs and the A54 preadipocyte cell line, which induce strong T cell suppression in Th1, produce high levels of NO in Th1 condition. These results suggest that NO also plays a major role in the preferential suppression of Th1 proliferation by MSCs.

To determine what inhibits the production of NO in Th1 condition, the two differentiation factors that support Th1 differentiation, anti-IFN-γ antibody and IL-4, were investigated. As a result, anti-IFN-γ antibody clearly inhibited the production of NO, whereas suppression by IL-4 was less evident. These results suggest that IFN-γ is a key regulator of NO production by MSCs.

Interestingly, cell supernatant collected from activated T cells had the ability to induce NO production by MSCs. IFN-γ is critical for NO production; however, in a T cell free environment, IFN-γ alone does not induce NO production from primary MSCs. IFN-γ in combination with LPS but not IL-2, stimulates NO secretion from primary MSCs, suggesting that both the IFN-γ and the signal from Toll-like receptor-4 (TLR4) are required for NO induction by MSCs. The addition of flagellin induced NO production in combination with IFN-γ. While, synthetic double strand RNA, poly(I:C), and CpG-oligonucleotide did not induce NO. Flagellin is a protein component of bacteria known to induce NO production from macrophages via TLR5 in the presence of either a TLR4 or IFN-γ signal. In addition to these factors, IL-1β and TNF-α induce NO when provided in combination with IFN-γ. As NF-κB is a downstream target of the signaling cascades activated by LPS, flagellin, IL-1β, and TNF-α, we hypothesized that activation of NF-κB is required for NO induction by MSCs. Bay-11-7085, a specific inhibitor of NF-κB, suppressed induction of iNOS in MSCs, thus suggesting that NF-κB is involved in NO production by MSCs as well as IFN-γ [20].

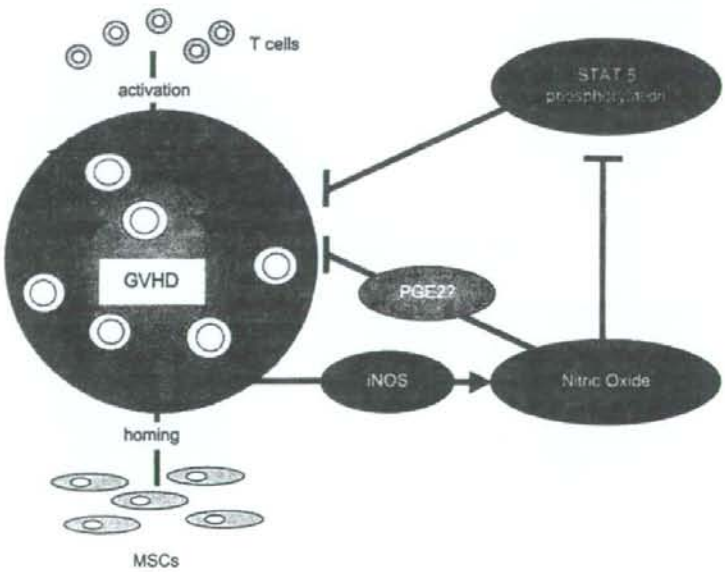

Fig. 2. MSC treatment of acute GVHD and the molecular mechanisms of T-cell suppression. MSCs are considered to accumulate at the site of inflammation and systemic adverse effects may not appear due to the local production of NO, which has very short half-life.

5. Retroviral vector-producing mesenchymal stem cells for tumor tracking and therapeutic gene amplification in suicide cancer gene therapy

MSCs are known to have a tendency to accumulate at the site of tumors, and therefore can be utilized as a platform for targeted delivery of anti-cancer agents [21–23]. The MSC-based targeted cancer gene therapy can enhance the therapeutic efficacy, because MSCs are considered to reach tumors including metastatic lesions and to deliver therapeutic molecules in a concentrated fashion. This targeted therapy can also reduce systemic adverse side effects, because the anti-cancer agents act locally at the site of tumors without elevating their systemic concentrations. We developed genetically-modified MSCs that produce retroviral vectors encoding HSV*tk*, aiming at augmenting therapeutic efficacy of systemic suicide cancer gene therapy (Fig. 3). The tumor tropism and anti-tumor effects of vector-producing MSCs (VP-MSCs) were examined by intravascular injection in tumor-bearing nude mice. MSCs isolated from the bone marrow of SD rats were transfected with plasmid DNA expressing luciferase alone (=non-VP-MSCs) or whole retroviral vector components (LTR-Luc or LTR-HSV*tk* with Gag-pol and VSV-G) (=VP-MSCs) by nucleofection. To assess tumor tropism of MSCs, nude mice were subcutaneously inoculated with 9 L rat glioma cells or Rat-1 fibroblasts, and were subsequently injected with luciferase-expressing MSCs through the left ventricular cavity. The transgene expression was periodically traced by using an *in vivo* imaging system. As a result, the transgene expression accumulated at the site of subcutaneous 9 L tumors, but undetectable at the site of Rat-1 fibroblasts. In addition, the injection of luciferase-expressing VP-MSCs caused much stronger signal of bioluminescence at the site of 9 L tumors compared with luciferease-expressing non-VP-MSCs. Immunostaining study showed that luciferase-positive cells (injected MSCs and transduced glioma cells) were detected at the periphery of tumors. To evaluate the therapeutic efficacy, tumor-bearing nude mice were treated with non-VP-MSCs or VP-MSCs combined with HSV*tk*/GCV system and then the size of subcutaneous tumors was periodically measured. In this model experiments, tumor growth was more efficiently suppressed by injecting VP-MSCs compared with non-VP-MSCs (Uchibori R, et al.: manuscript in preparation). This study suggests the effectiveness of VP-MSCs in suicide cancer gene therapy. The therapeutic benefit of this strategy should be further examined in orthotopic and metastatic tumor models.

6. Site-specific insertion of a therapeutic gene into the AAVS1 locus (19q13.4) in human mesenchymal stem cells by using adeno-associated virus integration machinery

Hematopoietic stem cells, ES cells, and MSCs are attractive targets for gene therapy and regenerative medicine, since they replicate themselves and differentiate into various cell lineages. To introduce genes in these stem cells, it is especially important to utilize a system that results in a minimal risk of insertional mutagenesis. To date, only one animal virus, the adeno-associated virus (AAV), is able to integrate into a defined site in human chromosome, AAVS1 (19q13.4), which is mediated by the activity of specific replicase/integrase protein, Rep. The Rep78 or Rep68 protein recognizes the GAGC motif on the viral inverted terminal repeat (ITR) sequence and a similar motif in AAVS1, leading to the site-specific integration of the AAV genome.

We and others have reported that a plasmid transfection system utilizing AAV derived components, the *rep* gene and ITR, could integrate the gene of interest preferentially into AAVS1 in epithelial or adherent cells (e.g., 293, HeLa, Huh-7 cells) [24–26]. Our system uses two plasmids, one harboring the transgene cassette flanked by the ITR sequences, and the other for *rep* expression, allowing only plasmid DNA harboring the ITR to integrate into the AAVS1 locus. In addition, this system can deliver DNA segments larger than the 4.5-kb packaging limit of AAV. As a first step toward establishing a method capable of integrating therapeutic DNA into the AAVS1 locus in MSCs, we tested this strategy in KM-102 cells, a cell line derived from human marrow stromal cells. KM-102 cells were co-transfected with a bicistronic plasmid containing a humanized GFP gene and a blasticidin S resistance gene (*bsr*) between the ITRs and a Rep68 plasmid. After transfection, single cell clones were grown in the presence of

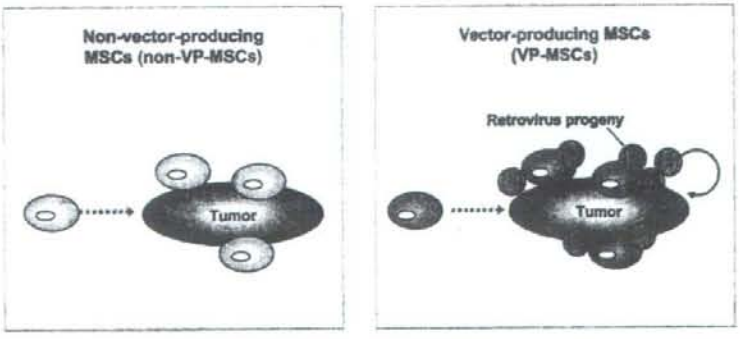

Fig. 3. Development of vector-producing tumor-tracking MSCs to augment suicide cancer gene therapy.

blasticidin S. Southern blot analysis of their genomic DNA revealed that three out of eight blasticidin S resistant clones showed site-specific integration of transgene into the AAVS1 site and that these clones had the GFP gene only at AAVS1. These results indicated that foreign DNA linked with ITR sequence could be targeted specifically into AAVS1 in KM-102 cells.

It is reported that the genome of myosin binding subunit 85 (MBS85) overlaps with the AAVS1 site [27]. To identify the junction between the transgene plasmid and the AAVS1 site, PCR was conducted using a transgene- and an AAVS1-specific primers. In two of the three clones the integration site was identified. In one clone the GFP gene was inserted at the first intron of MBS85 gene. The other clone had insertion of the GFP gene upstream of the first exon. Quantification of mRNA for MBS85 by real time PCR showed that the mRNA level decreased in these two KM-102 clones. The MBS85 is involved in the assembly of actin cytoskeleton. Although the outcome of allelic disruption of the MBS85 genome should be carefully evaluated, the system for AAVS1-specific integration of therapeutic DNA using AAV integration machinery is particularly valuable for *ex vivo* gene therapy applications for stem cells, such as ES cells and MSCs. For additional readings on the use of bone marrow cells for the treatment of autoimmunity, the reader is referred to companion papers published herein in this special issue of the Journal of Autoimmunity [28–38].

References

[1] Pittenger MF, Mackay AM, Beck SC, Jaiswal RK, Douglas R, Mosca JD, et al. Multilineage potential of adult human mesenchymal stem cells. Science 1999;284:143–7.

[2] Maitra B, Szekely E, Gjini K, Laughlin MJ, Dennis J, Haynesworth SE, et al. Human mesenchymal stem cells support unrelated donor hematopoietic stem cells and suppress T-cell activation. Bone Marrow Transplant 2004;33:597–604.

[3] Le Blanc K, Rasmusson I, Sundberg B, Götherström C, Hassan M, Uzunel M, et al. Treatment of severe acute graft-versus-host disease with third party haploidentical mesenchymal stem cells. Lancet 2004;363:1439–41.

[4] Ringden O, Uzunel M, Rasmusson I, Remberger M, Sundberg B, Lonnies H, et al. Mesenchymal stem cells for treatment of therapy-resistant graft-versus-host disease. Transplantation 2006;81:1390–7.

[5] Horwitz EM, Prockop DJ, Fitzpatrick LA, Koo WW, Gordon PL, Neel M, et al. Transplantability and therapeutic effects of bone marrow-derived mesenchymal cells in children with osteogenesis imperfecta. Nat Med 1999;5:309–13.

[6] Bang OY, Lee JS, Lee PH, Lee G. Autologous mesenchymal stem cell transplantation in stroke patients. Ann Neurol 2005;57:874–82.

[7] Nishikawa M, Ozawa K, Tojo A, Yoshikubo T, Okano A, Tani K, et al. Changes in hematopoiesis-supporting ability of C3H10T1/2 mouse embryo fibroblasts during differentiation. Blood 1993;81:1184–92.

[8] Oh I, Ozaki K, Miyazato A, Sato K, Meguro A, Muroi K, et al. Screening of genes responsible for differentiation of mouse mesenchymal stromal cells by DNA microarray analysis of C3H10T1/2 and C3H10T1/2-derived cell lines. Cytotherapy 2007;9:80–90.

[9] Sakamoto K, Yamaguchi S, Ando R, Miyawaki A, Kabasawa Y, Takagi M, et al. The nephroblastoma overexpressed gene (NOV/ccn3) protein associates with Notch1 extracellular domain and inhibits myoblast differentiation via Notch signaling pathway. J Biol Chem 2002;277:29399–405.

[10] Lijnen HR, Alessi MC, Van Hoef B, Collen D, Juhan-Vague I. On the role of plasminogen activator inhibitor-1 in adipose tissue development and insulin resistance in mice. J Thromb Haemost 2005;3:1174–9.

[11] Lassar AB, Buskin JN, Lockshon D, Davis RL, Apone S, Hauschka SD, et al. MyoD is a sequence-specific DNA binding protein requiring a region of myc homology to bind to the muscle creatine kinase enhancer. Cell 1989;58:823–31.

[12] Mackawa TL, Takahashi TA, Fujihara M, Urushibara N, Kadowaki-Kikuchi E, Nishikawa M, et al. A novel gene (drad-1) expressed in hematopoiesis-supporting stromal cell lines, ST2, PA6 and A54 preadipocytes: use of mRNA differential display. Stem Cells 1997;15:334–9.

[13] Mazini L, Wunder E, Sovalat H, Bourderont D, Baerenzung M, Bachorz J, et al. Mature accessory cells influence long-term growth of human hematopoietic progenitors on a murine stromal cell feeder layer. Stem Cells 1998;16:404–12.

[14] Arai F, Hirao A, Ohmura M, Sato H, Matsuoka S, Takubo K, et al. Tie2/angiopoietin-1 signaling regulates hematopoietic stem cell quiescence in the bone marrow niche. Cell 2004;118:149–61.

[15] Di Nicola M, Carlo-Stella C, Magni M, Milanesi M, Longoni PD, Matteucci P, et al. Human bone marrow stromal cells suppress T-lymphocyte proliferation induced by cellular or nonspecific mitogenic stimuli. Blood 2002;99:3838–43.

[16] Meisel R, Zibert A, Laryea M, Gobel U, Daubener W, Dilloo D. Human bone marrow stromal cells inhibit allogeneic T-cell responses by indoleamine 2,3-dioxygenase-mediated tryptophan degradation. Blood 2004;103:4619–21.

[17] Aggarwal S, Pittenger MF. Human mesenchymal stem cells modulate allogeneic immune cell responses. Blood 2005;105:1815–22.

[18] Albina JE, Abate JA, Henry Jr WL. Nitric oxide production is required for murine resident peritoneal macrophages to suppress mitogen-stimulated T cell proliferation: role of IFN-gamma in the induction of the nitric oxide-synthesizing pathway. J Immunol 1991;147:144–8.

[19] Sato K, Ozaki K, Oh I, Meguro A, Hatanaka K, Nagai T, et al. Nitric oxide plays a critical role in suppression of T cell proliferation by mesenchymal stem cells. Blood 2007;109:228–34.

[20] Oh I, Ozaki K, Sato K, Meguro A, Tatara R, Hatanaka K, et al. Interferon-gamma and NF-kappaB mediate nitric oxide production by mesenchymal stromal cells. Biochem Biophys Res Commun 2007;355:956–62.

[21] Studeny M, Marini FC, Dembinski JL, Zompetta C, Cabreira-Hansen M, Bekele BN, et al. Mesenchymal stem cells: potential precursors for tumor stroma and targeted-delivery vehicles for anticancer agents. J Natl Cancer Inst 2004;96:1593–603.

[22] Nakamizo A, Marini F, Amano T, Khan A, Studeny M, Gumin J, et al. Human bone marrow-derived mesenchymal stem cells in the treatment of gliomas. Cancer Res 2005;65:3307–18.

[23] Hall B, Dembinski J, Sasser AK, Studeny M, Andreeff M, Marini F. Mesenchymal stem cells in cancer: tumor-associated fibroblasts and cell-based delivery vehicles. Int J Hematol 2007;86:8–16.

[24] Surosky RT, Urabe M, Godwin SG, McQuinston SA, Kurtzman GJ, Ozawa K, et al. Adeno-associated virus Rep proteins target DNA sequences to a unique locus in the human genome. J Virol 1997;71:7951–9.

[25] Kogure K, Urabe M, Mizukami H, Kume A, Sato Y, Monahan J, et al. Targeted integration of foreign DNA into a defined locus on chromosome 19 in K562 cells using AAV-derived components. Int J Hematol 2001;73:469–75.

[26] Urabe M, Obara Y, Ito T, Mizukami H, Kume A, Ozawa K. Targeted insertion of transgene into a specific site on chromosome 19 by using adeno-associated virus integration machinery. In: Bertolotti R, Ozawa K, editors. Progress in gene therapy – vol. 3: autologous and cancer stem cell gene therapy. Singapore: World Scientific Publishing Co; 2007. p. 19–46.

[27] Dutheil N, Yoon-Robarts M, Ward P, Henckaerts E, Skrabanek L, Berns KI, et al. Characterization of the mouse adeno-associated virus AAVS1 ortholog. J Virol 2004;78:8917–21.

[28] Abraham N, Li M, Vanella L, Peterson S, Ikehara S, Asprinio D. Bone marrow stem cell transplant into intra-bone cavity prevent Type 2 diabetes: role of heme oxygenase and CO. J Autoimmunity 2008;30:128–35.
[29] Boren E, Cheema G, Naguwa S, Ansari A, Gershwin M. The emergence of progressive multifocal leukoencephalopathy (PML) in rheumatic diseases. J Autoimmunity 2008;30:90–8.
[30] Burt R, Craig R, Cohen B, Suffit R, Barr W. Hematopoietic stem cell transplantation for autoimmune diseases: what have we learned? J Autoimmunity 2008;30:116–20.
[31] Deane S, Meyers F, Gershwin M. On reversing the persistence of memory: hematopoietic stem cell transplant for autoimmune disease in the first ten years. J Autoimmunity 2007;2008(30):180–96.
[32] Gershwin M. Bone marrow transplantation, refractory autoimmunity and the contributions of Susumu Ikehara. J Autoimmunity 2008;30:105–7.
[33] Hara M, Murakami T, Kobayashi E. In vivo bioimaging using photogenic rats: fate of injected bone marrow-derived mesenchymal stromal cells. J Autoimmunity 2008;30:163–71.
[34] Ikehara S. A novel method of bone marrow transplantation (BMT) for intractable autoimmune diseases. J Autoimmunity 2008;30:108–15.
[35] Marmont A. Will hematopoietic stem cell transplantation cure human autoimmune diseases? J Autoimmunity 2008;30:145–50.
[36] Ratajczak M, Zuba-Surma E, Wysoczynski M, Wan W, Ratajczak J, Kucia M. Hunt for pluripotent stem cell – regenerative medicine search for almighty cell. J Autoimmunity 2008;30:151–62.
[37] Rezvani A, Storb R. Separation of graft-vs.-tumor effects from graft-vs.-host disease in allogeneic hematopoietic cell transplantation. J Autoimmunity 2008;30:172–9.
[38] Sonoda Y. Immunophenotype and functional characteristics of human primitive CD34-negative hematopoietic stem cells: the significance of the intra-bone marrow injection. J Autoimmunity 2008;30:136–44.

Gene 432 (2009) 7–18

Contents lists available at ScienceDirect

Gene

journal homepage: www.elsevier.com/locate/gene

Genomic organization of regions that regulate chicken glycine decarboxylase gene transcription: Physiological and pathological implications

Hiroshi Kawaguchi, Soshi Okamoto [1], Dwaipayan Sikdar, Akihiro Kume [2], Fang Li [3], Omar Mahmoud Mohamed Mohafez, Mohammed Hassan Shehata, Koichi Hiraga *

The Department of Biochemistry, University of Toyama Graduate School of Medicine and Pharmaceutical Sciences, 2630 Sugitani, Toyama 930-0194, Japan

ARTICLE INFO

Article history:
Received 31 July 2008
Received in revised form 5 November 2008
Accepted 7 November 2008
Available online 24 November 2008

Received by A. Bernardi

Keywords:
Promoter
Upstream regulator regions
Cell-type specificity
Glycine catabolism
Active one-carbon
Nonketotic hyperglycinemia

ABSTRACT

Regions required for chicken glycine decarboxylase gene transcription were examined. A region between −82 and +22 (−82/+22) with motifs similar to binding sites for Sp1, NF-Y and CP2 was assigned to the proximal promoter active in both chicken hepatoma cell line, LMH, and hepatocytes in primary culture. In LMH cells, a genomic region, KX, between KpnI (−4155) and XbaI (−2113) sites changed promoter activity with the aid of four additional genomic regions termed upstream regulator regions for suppression (UpRS) and activation (UpRA) of transcription. Those precise segments are UpR1S (−376/−346), UpR1A (−345/−291), UpR2S (−137/−108) and UpR2A (−107/−83). Within KX, −4155/−3605 activates and −3604/−3367 suppresses the promoter. −3366/−3024 activates or suppresses the promoter, probably with different UpR counterparts. −2197/−2113 restores the actions of −3366/−3024. While in LMH cells, the upstream UpRs abrogate the functions of immediately downstream UpRs, UpR1S or UpR2S or both may be at least less active in hepatocytes than in LMH cells. Nuclear extracts from various chicken tissues and LMH cells had UpR2A binding proteins in different populations, suggesting that together with the UpRs, the segments in KX are involved in the regulation of cell type-specific transcription of this gene.

1. Introduction

Glycine decarboxylase (GDC) [EC 1.4.4.2] (Hiraga and Kikuchi, 1980a,b), which was initially termed P-protein as reviewed by Kikuchi and colleagues (Kikuchi, 1973; Kikuchi and Hiraga, 1982; Kikuchi et al., 2008) constitutes the glycine cleavage system together with two other intrinsic components, the carrier protein of an aminomethyl group and hydrogen (H-protein) and tetrahydrofolate-requiring protein (T-protein), and a common lipoamide dehydrogenase. GDC, which catalyzes the initial decarboxylation of oxidative glycine degradation, requires two types of functions of H-protein. First, GDC, a potential enzyme by itself, is converted to an active decarboxylase by H-protein. Second, the decarboxylation product, aminomethyl carbanion, is captured by the prosthetic lipoyl moiety of H-protein in association with the reductive cleavage of its disulfide bond for further breakdown to NH_3 and N^5, N^{10}-methylene-tetrahydrofolate by T-protein (Hiraga and Kikuchi, 1980b; Kikuchi and Hiraga, 1982; Kikuchi et al., 2008). The reaction catalyzed by T-protein finally yields the reduced form of the prosthetic lipoic acid, which is recycled through oxidation by lipoamide dehydrogenase in the presence of NAD^+. This overall reaction is the major pathway for glycine degradation in vertebrates (Kikuchi, 1973) and supplies tetrahydrofolate derivatives indispensable for the biosynthesis of purine nucleotides, thymidylate, methionine, lipids and other cellular substances.

Livers of uricotelic animals exhibit the highest specific activity of glycine cleavage reaction in the vertebrate tissues examined (Kikuchi, 1973; Kikuchi et al., 2008; Kure et al., 1991a,b), probably because purines are involved in the pathway for NH_3 excretion. In chicken tissues, the specific activity of glycine cleavage reaction was determined in the liver, kidney, and brain in a ratio of 100:30:3. GDC mRNA levels in these tissues were proportional to this ratio. Heart and spleen tissues are inactive in glycine cleavage reaction due to negligible levels of GDC. Run-on transcription analysis revealed that the tissue-specific GDC levels are predominantly determined at the level of transcription (Kure et al., 1991a,b). In 16-day chick embryo livers, the levels of specific activity, polypeptide and mRNA of GDC were approximately 10% of those in adult chicken livers and began to increase at late embryonic stages. Eventually, GDC increased to the adult level after hatching due to increased transcription of the GDC gene (Matsui et al., 1993). In other words, GDC gene transcription may

Abbreviations: GDC, glycine decarboxylase; UpRA and UpRS, upstream regulator regions for activation and suppression of transcription.

* Corresponding author. Tel.: +81 76 434 7225; fax: +81 76 434 5014.
E-mail address: hiragak@med.u-toyama.ac.jp (K. Hiraga).
URL: http://www.med.u-toyama.ac.jp/bmb/index.html (K. Hiraga).
[1] Present address: The Department of Neurosurgery, University of Toyama School of Medicine, Japan.
[2] Present address: The Division of Genetic Therapeutics, Jichi Medical School, Tochigi 329-0498, Japan.
[3] Present address: Institute of Molecular Biosciences, Massey University, Palmerston North, New, Zealand.

0378-1119/$ – see front matter © 2008 Elsevier B.V. All rights reserved.
doi:10.1016/j.gene.2008.11.014

be increasingly changed in the embryonic and neonatal livers and constitutively maintained at the maximally increased level in the adult liver. Moreover, GDC gene transcription is less active in the kidney and brain than in the liver, and inactive in the heart and spleen. These properties imply that the availability of *trans*-factors required for GDC gene transcription regulation presumably changes in response to the statuses of tissue differentiation to provide conditions appropriate for glycine catabolism.

Concerning GDC gene structure, we characterized part of a 5′-exon in a chicken genomic DNA clone, pCPG301EE2.8 subcloned from λCPG301, to determine the translation start site, since the initially cloned chicken GDC cDNA was a truncated form with no translation start codon (Kume et al., 1991). The isolation of chicken GDC cDNA clones helped to clone a human version of GDC cDNA (Kume et al., 1991). Sakakibara et al. (1990) further clarified that the human genome possesses true and processed GDC genes, which were respectively assigned to 9p23–24 and 4q12 (Isobe et al., 1994). In humans, a defective glycine cleavage system causes nonketotic hyperglycinemia (Kikuchi, 1973; Kikuchi and Hiraga, 1982; Nyhan, 1989; Kikuchi et al., 2008). Most patients with this disease had a molecular lesion in GDC and therefore in its genes (Kume et al., 1988; Sakakibara et al., 1990; Kure et al., 1991a,b; Takayanagi et al., 2000; Kure et al., 2006; Kanno et al., 2007). Notably, Sakakibara et al. (1990) identified for the first time that the GDC gene of a patient with this disease had been deleted at a 5′-region. A recent study has confirmed that the deletion including a 5′-region of the human GDC gene is a major cause of nonketotic hyperglycinemia (Kanno et al., 2007). In this context, GDC genes have been identified from various micro-organisms (Wilson et al., 1993; Okamura-Ikeda et al., 1993; Nakai et al., 2005) and their structures can be seen in several databases. In *Escherichia coli*, a LysR family protein regulates the biosynthesis of the components of the glycine cleavage system (Wilson and Stauffer, 1994). In *Saccharomyces cerevisiae*, a genomic region with a core element, CTTCTT, was required for induction of the yeast homolog of GDC under nutritionally restricted conditions (Hong et al., 1999; Sinclair et al., 1996). However, regulation mechanisms directing vertebrate GDC gene transcription were largely unknown. Taking the features of chicken GDC gene transcription into account, we attempted to structurally and functionally characterize genomic regions that may be involved in chicken GDC gene transcription regulation.

2. Materials and methods

2.1. DNA clones, plasmids, cells and RNA

Chicken genomic DNA subclones constructed with pBluescript from λCPG301 (Fig. 1A) (Kume et al., 1991; Yamamoto et al., 1991) were used. A chicken hepatoma cell line, LMH (JCRB0237) (Kawaguchi et al., 1987), was obtained from the Health Science Research Resources Bank (Osaka, Japan) and maintained in Waymouth MB752/1 medium containing 10% fetal bovine serum at 37 °C and under 5% CO_2 in air. Chickens at 4 months of age were also used. Total RNA was prepared from chicken livers and LMH cells as described (Chomczynski and Sacchi, 1987). pGL3-basic and pRL-SV40 vectors (Promega Corp.) and other reagents were from local distributors.

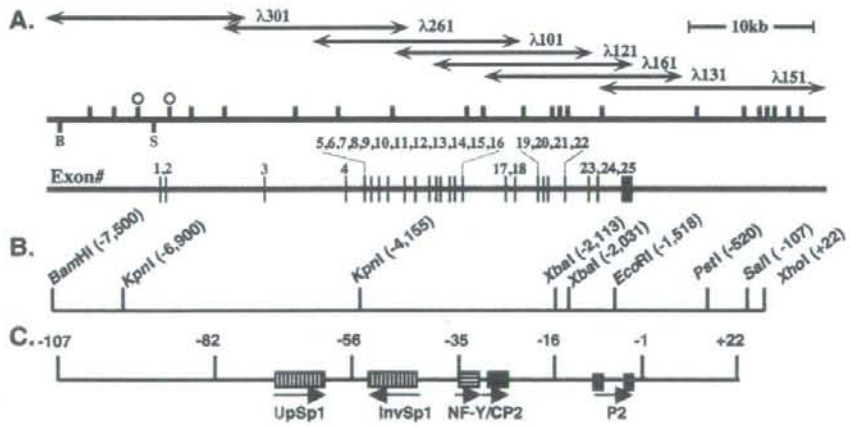

D.

```
-540 ctctgcccaa gccacctgca gatgttcact gtagggcact gtaaagattt tggtacaaag
-480 tgctgggcag tgttaaggga ttgaacactt cagatgaaga cacagcaatg catgtgtacg
-420 tacacagcag catcacagtg ccatcttaaa ctgctgggtc ctctgggaaa atttattagc
-360 gctgcaaaac taagagaaga tggaggctgt ggtggccctt tgcagcccag cagaattgca
-300 cactagatgg ccatcggtgg tgcggccagg cgcggtgcag ccttgccccc tcctcagaga
-240 tgcgcacaaa gcgccgggtg ggatgaatct ttccttatct gctccgacag ccccaggccg
-180 gagggcaacg caaagcccgg ccatctccgc atccccgcgc ggccggagcg gggtcagggc
-120 cgagcgggtc gggtcgactc ggccgggggc gtggggatca ggtggcggcg aggcgggggcg
 -60 agcgcggcac cgcctctcct ccccattggc gctggcggcg ggggccgcgc cgcaccgccc
  +1 TCCCCGGCCA CAAAGCGTGG TGCCGGACGG CGGCGGTGGG GCGGTGTTAG CGGGGTCATG
```

Fig. 1. Genomic organization of the chicken GDC gene. (A) The outline of the cloned GDC gene. Genomic DNA fragments of λclones (arrows), recognition sites for EcoRI on the DNA stretch (vertical graduations on the bold line), those for BamHI (B) at ~7.5 kb and SalI (S) at ~107, pCPGEE2.8 insert (the region between open circles), and locations of 25 exons in red are shown. (B) Recognition sites by several restriction enzymes are shown along with the 5′-flanking sequence. (C) Cis-elements in the proximal promoter. Positions (nucleotide numbering) and directions (arrows) are shown. UpSp1 and InvSp1 denote the inverted repeats of Sp1 sites. (D) The nucleotide sequence from −540 to +60. UpR1S (−376/−346) and UpR2S (−137/−108), and UpR1A (−345/−291) and UpR2A (−107/−83) are shown in blue and red, respectively. UpSp1 and InvSp1 are underlined. Lowercase and uppercase letters indicate the 5′-flanking region and part of exon 1. Translation start codon is from +58 to +60. Accession number of the nucleotide sequence from −4160 to −1 is AB245436.

2.2. Recombinant plasmids carrying promoter regions

The region between the BamHI and SalI sites within the λCPG301 insert (the region between B and S in Fig. 1A) was subcloned as pBS. Note that the pBS insert is referred to as the genomic region −7500/−108 in Table 2. The 5′ primer, 5′-GGG CCG AGC GGG TCG GGT CGA CTC GG-3′ (−124 to −99) encompassing the underlined internal SalI site at −107, and the 3′ primer complementary to a sequence from +1 to +22 of chicken GDC cDNA (5′-GGC TCG AGC ACC ACG CTT TGT GGC CGG GGA-3′) with the underlined artificial XhoI site were used to amplify the −107/+22 region on a pCPGEE2.8 template by PCR. A product subcloned at the EcoRV site in pBluescript in an appropriate orientation was cut at XhoI sites in the 3′ primer and multiple cloning sites to remove a SalI site between them. The insert of the self-ligation product (pSX) was termed −107/+22. The pBS insert was transferred to pSX using BamHI and SalI sites, yielding a subclone carrying the 7.5-kb-long genomic region upstream from +22. The required flanking regions between appropriate sites for restriction enzymes (see Fig. 1B) and the XhoI site were subcloned with a pGL3-basic vector. −107/+22 in the pGL3 vector was unidirectionally deleted by the method of Henikoff (1984) to prepare subclones each carrying −82/+22, −56/+22, and −35/+22. Nucleotide sequences were determined using various synthetic DNA primers and an automated DNA sequencer, Prism 310 (Applied Biosystems Japan).

2.3. Transcription start site

Primer 1 (5′-GCG CCC GCA GCT CTG CAT GA-3′) (Tm=58 °C in 75 mM KCl) was synthesized as a strand complementary to chicken GDC mRNA. Its 5′-end base is complementary to that 18 bases downstream from the adenine base of the translation start codon in the reported chicken GDC cDNA sequence (Kume et al., 1991) and to that at +75 in the complete exon 1 sequence determined in the present study. The CAT near the 3′-end of primer 1 is complementary to the translation start codon shown in Fig. 1D. The 5′-end of 20-mer primer 2 was 123 bp downstream from that of primer 1. Primer extension (Calzone et al., 1987) was performed with 5′-end-labeled primer 1 or 2 ([^{32}P]-primer 1 or 2), chicken liver total or poly(A)$^+$ RNA (20 to 2 μg) and a reverse transcriptase. For S1 protection assay, a 182-base-long single-strand DNA probe was replicated from [^{32}P]-primer 1 on a pCPG301EE2.8 template cleaved in advance at the −107 SalI site. The probe DNA was separated from the template plasmid by electrophoresis on a gel containing 7 M urea. The probe DNA was annealed at 60 °C for 2 h with liver poly(A)$^+$ RNA (2 μg) denatured in advance at 90 °C for 2 min, and then digested with S1 nuclease (5 U/ml) for 5 to 90 min at 37 °C. Products from primer extension and S1 protection reactions were simultaneously resolved on the denatured gel together with aliquots of mixtures for sequencing reactions that also began with [^{32}P]-primer 1 on the pCPG301EE2.8 insert. Products were located on XAR5 films (Kodak) or a BAS2000 imaging analyzer (Fuji Film Co. Ltd., Tokyo).

2.4. Electrophoretic mobility shift assay

Nuclear fractions isolated from LMH cells and chicken livers (Hibino et al., 2006) were extracted with a buffer containing 0.3 M NaCl by the method of Dignam et al. (1983) and stored at −80 °C until use in electrophoretic mobility shift assay (EMSA). Aliquots of the nuclear extract (1 to 5 μg in protein amounts) were incubated with radioactive genomic or synthetic DNA probes (20,000 cpm) for 20 min at room temperature in a reaction mixture containing, in a final volume of 15 μl, 10 mM Tris–HCl buffer, pH 7.5, 40 mM NaCl, 1 mM EDTA, 1 mM dithiothreitol, 6 mM $ZnCl_2$, 0.4 μg of poly [dI-dC], 0.5 mM PMSF, and 4% glycerol (Hennighausen and Lubon, 1987). For competition assay, the nuclear extract was treated with 200 molar excess competitors at room temperature for 20 min prior to addition of [^{32}P]-DNA probes. DNA/protein complexes were resolved on a 4% polyacrylamide gel containing 6.7 mM Tris–HCl buffer, pH 7.5, 3.3 mM sodium acetate, and 1 mM EDTA and located on autoradiograms.

2.5. Site-directed mutagenesis

Base substitutions were introduced using a Mutan-Super Express Km kit (Takara Bio, Japan) according to manufacturer's instructions. The mutants with a confirmed nucleotide sequence were used for promoter assays. Double-stranded UpR2A sequences with three-nucleotide substitutions were chemically synthesized for use in EMSA or ligated with −82/+22 in a pGL3-basic vector to prepare mutant −107/+22 constructs.

2.6. Chick hepatocyte primary culture

This was performed by the method of Seglen (1976). Chicks at 5 weeks of age were anesthetized and killed by cervical incision. The liver was perfused with 250 ml of Mg^{2+}- and Ca^{2+}-free Hanks' solution, followed by perfusion with 400 ml of HEPES-NaOH buffered saline (pH7.5) containing 50 mg/ml of collagenase at 37 °C. Dispersed cells were suspended with Hanks' solution. Hepatocytes collected by centrifugation at 60 ×g for 2 min were dispersed with Waymouth MB752/1 medium containing 10% fetal bovine serum, and maintained with the medium supplemented with 10 μM dexamethasone and 100 nM insulin under 5% CO_2 in air at 37 °C for 9 days by changing the culture medium at 24-h intervals to assay for promoter activity in hepatocytes.

2.7. Transient expression of luciferase gene

Wild-type and recombinant pGL3-basic and pRL-SV40 vectors were isolated by CsCl equilibrium centrifugation and transfected to LMH cells and hepatocytes by lipofection using Tfx-50 (Promega Corp.). Four cultures of LMH cells and hepatocytes received identical constructs under comparable conditions and were respectively lysed following 40 h- and 72 h-incubations. The lysates were assayed for firefly and *Renilla* luciferase on a Dual-luciferase Reporter Assay System (Promega Corp.) and a luminometer, Luminous CT-9000 (DiaYatron, Tokyo). Promoter activities were expressed as a mean value of four assays ± SD.

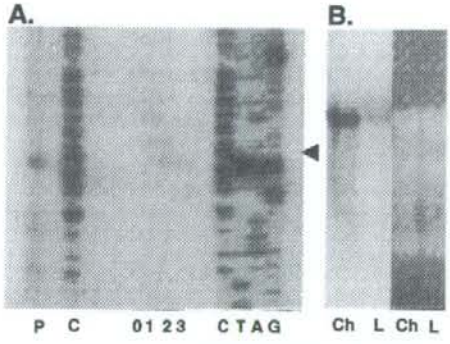

Fig. 2. Transcription start site. (A) The product extended from [^{32}P]-primer 1 (lane P) and the single-strand DNA probe prepared from [^{32}P]-primer 1 and protected from S1 nuclease digestion for 0, 30, 60, and 90 min (lanes 0, 1, 2, and 3) were resolved by electrophoresis on a denatured gel. Sequencing ladders also begin with [^{32}P]-primer 1 (lanes C, T, A, G). An arrowhead indicates thymine base at the transcription start site. (B) Northern blot analysis. Chicken liver (lane Ch) and LMH cell (lane L) total RNA (10 μg) were probed with [^{32}P]-GDC cDNA (left). RNA staining with ethidium bromide is shown (right).

Table 1
Boundary sequences of 25 exons

Exon/intron boundary sequence			
Exon	(bp)	5′ End	3′ End
1	282	cgcaccgcccTCCCCGGCCA	CGGGGTGCAGgtgggtgcct
2	79	ttctttgcagAGCGTCGAGG	GACCACGTCGgtaaattgcc
3	136	tctcaattagTTGAAAATGA	ACGCAGGATGgtaatgtaca
4	165	ttccttacagGGTTACCCAG	TATGTCACAGgtactatgtt
5	76	tttttaacagGCAAAACAAA	CTAGAGCAAAgtatgttctt
6	148	tgtttttccagTTATACAGGT	TCAGAATGGGgtaaagtaaa
7	197	ccctcctcagACTCTTGCCT	GCGTTACAAGgtaaaggctc
8	97	tgtgtcttagAGATGCAAAT	CACTGCACAGgtgactcatc
9	106	ggatccttagGCTCTCCTGG	CTGGCGGAGGgtcgaatatt
10	140	tgttttatagGTCTCAGACG	TGATGGCAGAgtaagcaacc
11	81	ttgcccatagCTTGGAGTAT	GTCTTCAGCTgtaagtggac
12	98	tgtgtcaaagGAACTAGTTG	TTTTCAACAGgttttgtgaa
13	85	tgtcctccagCTATCACTCC	GATTCCTTTGgtgggtattt
14	42	ctatttttagGGGTCCTGTA	TGAACTTGCGgtaagttgaa
15	143	tttgtttaagCCGATTTCAT	AACCAAACAGgtaggaattt
16	76	cctcttgcagTGGAGCCCAA	TCATAGAAGTgtaagtgtca
17	126	tccttccaagGTTTGCCTTA	AAAAGCAATGgtgagtattt
18	150	ctgcctccagGTGGACAAGC	GAATGCACAGgtatgcagtc
19	113	cactttacagGTGGGTCTGT	CAATTGGAGTgtaagtatat
20	142	tttgttttagGAAGAAACAT	GTATATCAAGgtgtgtagac
21	112	ctcttttcagACAATGGGAG	GGAGTAAGAGgcaagtagtg
22	96	ttccttacagGTTACGTAGC	CAGGATTATGgttagtcaaa
23	173	ctgttttcagGTTTTCATGC	CCCTCTGAAGgtaagatggc
24	81	ctgcttgcagATGTCACCAC	ATTCCCACTGgtgagtaaac
25	628	ctgcatttagCCTTTTGTGA	GGTCAGAATTaagtatcatg

Exon/intron boundary sequences are shown for all exons (uppercase letters), and 5′-flanking sequence and introns (lowercase letters) together with the lengths of exons in bp. Chicken GDC cDNA sequence can be seen with accession numbers D90266, M64402 or NM_204322.

2.8. Chicken GDC gene locus

AB245436 is a 4220 bp chicken genomic sequence between the KpnI site at −4155 (Fig. 1C) and the 3rd base of the translation initiation codon in exon 1 (Fig. 1D). Various segments of AB245436 and a chicken cDNA sequence (NM_204322) were aligned over chicken genomic regions using tools, Blat and Blast, accessible from the UCSC Genome Bioinformatics Site (http://genome.ucsc.edu/) and National Center for Biotechnology Information (http://blast.ncbi.nlm.nih.gov/Blast.cgi). Deposits related to ENSGALG00000015053 that identifies the chicken gene for GCSP were examined for the correctness, since GCSP is an alternative name of GDC of the glycine cleavage system. Human and chicken genome databases were also searched using the two tools for sequences similar to the chicken UpRs. Putative *cis*-elements were searched using a tool, Patch, at gene-regulation. com (http://www.gene-regulation.com/).

3. Results

3.1. Transcription start site

In the previous study, we determined that the translation start codon was downstream from the unique SalI site in a 2.8-kb chicken GDC gene fragment subcloned from λCPG301 as pCPG301EE2.8 (the region between open circles in Fig. 1A) (Kume et al., 1991). In the present study, we tried to determine the transcription start site and exon/intron boundaries of this gene. In primer extension analysis using chicken liver total RNA, a major 75-base-long product (lane P in Fig. 2A) was reverse-transcribed from [^{32}P]-primer 1. Under comparable conditions but using chicken liver poly(A)$^+$ RNA, an approximately 200-base-long product extended from [^{32}P]-primer 2 (not shown). The two products were thought to extend to similar endpoints on GDC mRNA, since primer 2 begins with the base 123 bases downstream from the 5′-end of primer 1. For S1 nuclease mapping, a 182-base-long single-stranded genomic DNA was replicated from [^{32}P]-primer 1 to the SalI site on pCPG301EE2.8 (see Experimental Procedures) and annealed with liver poly(A)$^+$ RNA. The 75 bases long product was again protected from digestion of the hybrid with S1 nuclease. Its signal intensity clearly increased accordingly to the prolonged digestion (Fig. 2A, lanes 0, 1, 2, and 3). The products from primer extension and S1 protection assays electrophoretically migrated to a position corresponding to the thymine base indicated with an arrowhead beside the sequencing ladders, which also begin from [^{32}P]-primer 1. These findings imply that chicken GDC gene transcription may mainly begin with this thymine base that is 57 bases upstream from the adenine nucleotide of the translation start codon in exon 1 (Fig. 1D), although at present we cannot rule out the possibility that GDC gene transcription starts at multiple sites (cf. Gustincich et al., 2006). Transcription start site determination and comparison of GDC cDNA sequence with genomic sequences of the clones shown in Fig. 1A revealed that this gene has 25 exons comprising 3572 bases in a 40-kb-long genomic region (Fig. 1A and Table 1). In a 7.5-kb-long region flanking the 5′-end of exon 1, KpnI

Table 2
Identification of the proximal promoter and its important *cis*-elements

Experiment 1		Experiment 2[a]				
Genomic region	Relative luciferase activity	Genomic region	Binding site	Name	Mutant sequence	Relative luciferase activity
−7500/+22[b]	40.7±6.0	−107/+22	CP2	WT	-16 CCGCGCCCGCACCGC -3	33.0±3.4
−4155/+22	27.3±2.3			M1	-16 ACGTGCCGCACCGC -3	36.6±3.6
−2113/+22	37.5±6.3			M2	-16 CGCGCCGCAACGT -3	26.1±2.4
−1518/+22	32.4±9.9			M3	-16 CCGCGCCGCAACAT -3	28.7±2.4
−520/+22	39.0±7.8			M4	-16 ACATGCCGCAACAT -3	16.4±1.3
−107/+22	25.9±4.6					
−7500/−108	1.0±0.1		NF-Y/CP2	WT	-36 ATTGGCGCTGG -26	33.0±3.4
				M5	-36 AATTCCGCTGG -26	29.4±9.7
−82/+22	19.7±3.5			M6	-36 ATTGGCGATGT -26	31.8±9.8
−56/+22	8.0±1.7					
−35/+22	1.2±0.3		UpSp1	WT	-71 GAGGCGGGGC -62	33.0±3.4
				M7	-71 GATTCGGGGC -62	7.5±0.1
pGL-3B[c]	1.0			M8	-71 GAGGCTA TAGGC -62	18.3±1.8
		−56/+22	InvSp1	WT	-54 GCACCGCCTC -45	33.0±3.4
				M9	-54 GCACCGAATC -45	20.7±2.6
			InvSp1	WT	-54 GCACCGCCTC -45	7.5±1.3
				M10	-54 GCACCGAATC -45	5.1±1.4

[a] −107/+22 and −56/+22 with mutagenized nucleotides (underlined) were defined as M1 to M10 and assayed for promoter activity. Relative luciferase activity was expressed as mean value±SD of four assays.

[b] In Experiment 1 and 2, promoter assay was performed using genomic regions prepared at the recognition sites for BamHI (−7500), downstream KpnI (−4155), upstream XbaI (−2113), EcoRI (−1518), PstI (−520), SalI (−107) and artificial XhoI (+22). Their relative positions are also shown with nucleotide numbering in Fig. 1B.

[c] pGL-3 basic vector.

(−4155), XbaI (−2113), EcoRI (−1518), PstI (−520) and SalI (−107) mapped their recognition sites, and base sequencing confirmed them at the parenthesized positions (Fig. 1B). The 5′-end BamHI site and the upstream KpnI site were mapped by electrophoresis at positions −7.5 and −6.9 kb distant from the major transcription start site (Fig. 1B). A nucleotide sequence including regions required for transcription regulation is shown in Fig. 1D. The codon for the active-site lysine residue (738K) of GDC resides in exon 19. Exon/intron boundaries of the chicken GDC gene resemble those of the human GDC gene, although the transcription start site of the chicken GDC gene differs by the definition adopted in structural analyses of the human GDC gene (Takayanagi et al., 2000).

3.2. The chicken GDC gene locus

Taking advantage of use of the AB245436 and NM_204322 for chicken GDC gene locus identification, we tried to align segments from the two sequences over chicken genomic DNA sequences. Blat analyses respectively assigned the first base of AB245436 (the first nucleotide of KpnI site at −4155) and the 3499th T immediately upstream from the first adenine base of poly(A) tail in the chicken GDC cDNA sequence in NM_204322 (the 3′-end of exon 25) to the bases at 28600582 and 28557830 in the chicken chromosome Z minus strand. However, a 3′-region of the AB245436 sequence and regions upstream from the 5′-end of exon 3 appeared to be defective in the UCSC database sequence. Another chicken chromosome Z sequence (accession number: AC202790) in High-Throughput Genomic Sequence Database (http://www.ncbi.nlm.nih.gov/HTGS/) had the defective region. In the AC202790 sequence, the 5′-end of the AB245436 sequence and the 3′-end of exon 25 corresponded to 198347 and 240569, encompassing a 42,222-base-long region in which there were 25 exonic sequences with the 5′- and 3′-ends basically similar to those shown in Table 1. Thus, the chicken GDC gene locus may reside in the chromosome Z minus strand. Database searches revealed that the entire sequences of UpR1S+UpR1A and UpR2S+UpR2A reside only in the chicken GDC gene locus. A segment −324/−302 of UpR1A is included in chicken chromosome 2 DNA as a coding region of an mRNA sequence (XM_418505). Similar region (−321 to −302) was present in chromosome 5 DNA (56222862–56222881). Concerning the ENSGALG00000015053 related sequence, exons 1 and 2 of the GCSP gene begin at positions near 5′-ends of the true exons 3 and 4 yielding a reading frame quite different from that in NM_204322.

3.3. Chicken GDC gene promoter

Serial deletion mutants of the 7.5-kb flanking region were unidirectionally prepared as regions between one of the six native cleavage sites by the restriction enzymes listed above and the artificial XhoI site at +22. These genomic regions were defined as −7500/+22, −4155/+22, −2113/+22, −1518/+22, −520/+22 and −107/+22 (Fig. 1B and Table 2) and ligated upstream from a reporter firefly luciferase gene in a pGL3-basic vector to assay for promoter activity in recipient LMH cells which had GDC mRNA at about 10% of its hepatic level in the adult chicken (lane L of the left panel in Fig. 2B). The cells transfected with one of the six constructs showed luciferase activity ranging from 26 to 40 in arbitrary units (Experiment 1 in Table 2). The −7500/−108 region that is identical to the pBS insert (see Materials and methods) was inactive, indicating that the proximal −107/+22 region is required for luciferase gene transcription. The most downstream region, −82/+22, which significantly increased luciferase activity (Experiment 1 in Table 2) was GC-rich (14 CpG pairs among 34C and 35G nucleotides within the −82/−1 region) and had neither a canonical TATA box (Breathnach and Chambon, 1981; Maniatis et al., 1987) nor an initiator sequence (Corden et al., 1980; Smale and Baltimore, 1989) (Fig. 1C and D). Instead, this region had several binding motifs for the following known *trans*-activators: upstream Sp1 (−71 to −62, UpSp1) and inverted Sp1 (−54 to −45, InvSp1) (Dynan and Tjian, 1983), NF-Y (−36 to −32, ATTGG) (Chodosh et al., 1988; Mantovani et al., 1992; van Huijsduijnen et al., 1990), and CP2 (−29 to −26 as CNRG, and −16 to −3 as CNRGN6CNRG) (Lim et al., 1993; Murata et al., 1998). The −82/+22, −56/+22, and −35/+22 regions, which are three serial deletion mutants of UpSp1, InvSp1 and part of the NF-Y motif, respectively exhibited 80%, 30% and 3% of luciferase activity exhibited by −107/+22.

3.4. Functional confirmation of the putative cis-elements

Experiment 2 in Table 2 summarizes results from functional examinations of pGL3-based constructs each carrying one or more motifs mutagenized in −107/+22 and −56/+22. The downstream CP2 motif with increasing numbers of base substitutions up to 6 bases (M1 to M4) decreased luciferase activity to 50% of that yielded by the wild-type −107/+22. Mutations in the NF-Y/CP2 motif were ineffective on promoter activity (M5 and M6). M7 with mutations in UpSp1 in −107/+22 lost 80% of the activity of the wild-type sequence. M8 with substitutions at different positions in UpSp1 of −107/+22 (GG at −66 and −65 to TA), and M9 with comparable mutations in InvSp1 in −107/

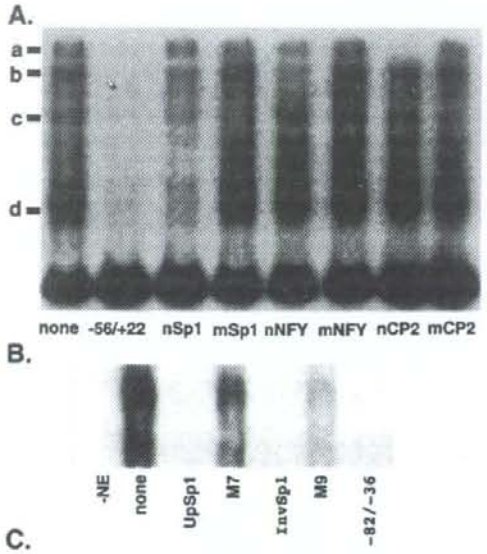

Competitor	Nucleotide sequence
nSp1	5′-ATTCGATCGGGGCGGGGCGAGC-3′
mSp1	5′-ATTCGATCGGTTCGGGGCGAGC-3′
nCP2	5′-AGCTGACCAGTTCCAGCCACTCTTTAGTC-3′
mCP2	5′-AGCTGAACATTTACATACACTCTTTAGTC-3′
nNF-Y	5′-GATCCCTTTTAACCAATCAGAAAAATGTG-3′
mNF-Y	5′-GATCCCTTTTAAGAATTCAGAAAAATGTG-3′
UpSp1	−82 CAGGTGGCGGCGAGGCGGGGCGAGCG −57
M7	−77 GGCGGCGATTCGGGGCGAGC −58
InvSp1	−36 GGGGAGGAGAGGCGGTGCCG −56
M9	−36 GGGGAGGAGATTCGGTGCCG −56

Fig. 3. Binding of proteins to the promoter. (A) EMSA using [^{32}P]-labeled −56/+22 and chicken liver nuclear extracts (10 μg). Letters a, b, c, and d verify major bands. Competitors are shown under each lane. (B) EMSA using −82/−57 probe. Conditions are similar to those used in (A). (C) Competitors used in (A) and (B). Motifs and mutagenized bases in native (n) and mutant (m) competitor sequences are underlined.

+22 were respectively 50% and 60% as active as the wild-type sequence. M10 prepared by introducing the mutations identical to those in InvSp1 of M9 into −56/+22 was 65% as active as the wild-type −56/+22, implying that UpSp1, InvSp1 and the downstream CP2 motifs are required for transcription activity.

3.5. The binding of proteins to the cis-elements

EMSA using liver nuclear extracts of chickens at 4 months of age and a [^{32}P]-labeled −56/+22 probe revealed four bands defined as a, b, c and d (Fig. 3A, lane "none" indicating none of the competitors), all of which were abrogated with the cold −56/+22 competitor (Fig. 3A, lane −56/+22). Native competitors for CP2 (lane nCP2), NF-Y (lane nNFY) and Sp1 (lane nSp1) respectively abrogated the bands a, b and d. Data indicate that InvSp1 actually binds an Sp1-like protein. The −82/−57 probe in which UpSp1 is present (Figs. 1C and 3C) yielded bands that were abrogated with both UpSp1 and InvSp1 competitors, whereas their mutants, M7 and M9, did not completely abrogated them (Fig. 3B). Therefore, UpSp1 is likely to be a binding site for an Sp1-like protein. The NF-Y/CP2 motifs formed DNA/protein complex (Fig. 3A), although their mutagenized motifs did not appear to clearly affect promoter activity (Table 2). Properties of band c are unclear at present, since it disappeared in response to mSp1 and mCP2 (Fig. 3A). We further tried to confirm immunochemical properties of the *trans*-factors. Western blot analysis, however, revealed that commercially available antibodies each specific to rodent Sp1, C/EBP-α and β and NF-Y were unreactive to chicken liver nuclear proteins. Taking the properties determined by promoter assays and EMSA into account, we assigned −82/+22 to the proximal promoter of the chicken GDC gene. As estimated by the difference in activity of −107/+22 from that of −82/+22 in Experiment 1 of Table 2, the −107/−83 region was thought to have an element that increases promoter activity.

3.6. Changes in promoter activity by upstream regions

To address whether the cloned 5′-flanking region has additional regions that change promoter activity, LMH cells were transfected with constructs in which appropriately cleaved 5′-flanking regions were directly ligated to −107/+22 (Fig. 4A). Of these, a construct carrying a region between a KpnI site at −4155 and an XbaI site at −2113 (we defined this region as KX) clearly increased luciferase activity in LMH cells (construct 4 in Fig. 4A), indicating that KX and −2113/−83 may have regions that change promoter activity. Actually, −520/−108 appeared to suppress the KX-dependent promoter activation (constructs 2 and 3 in Fig. 4B). Sequential removal of short segments within this region in the 5′ to 3′ direction, however, changed promoter activity in a somewhat more complicated manner as follows; in Fig. 4C, KX activity is detectable in the presence of −345/−292 (construct 4) and −107/+22 (construct 8), whereas

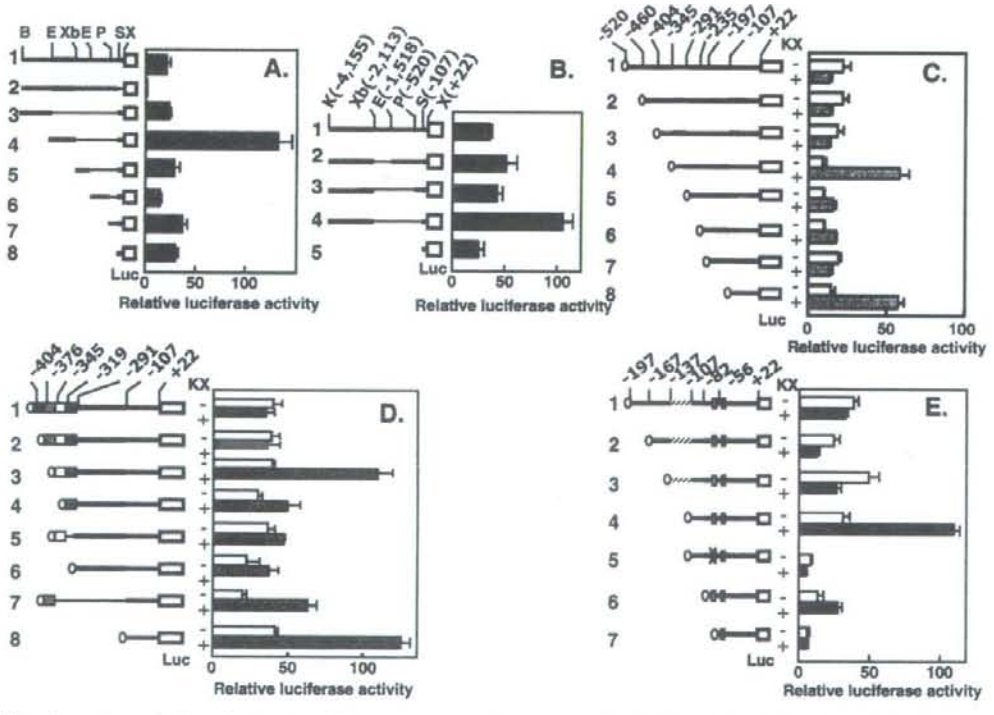

Fig. 4. KX-dependent promoter activation and its suppression by four UpRs. (A) Activation of the promoter by KX. The numbering verifies pGL3-basic vector-based constructs. The 5′-flanking region (bold line) was cut at sites shown over construct 1 (initials in uppercase letters). Various regions were ligated at the 5′-end of −107/+22 in a pGL3-basic vector to assay for promoter activity in LMH cells. (Luc) and (open box) denote a luciferase gene. Note that −107/+22 had been deleted in construct 2. (B) Regions that change promoter activity. −4155/−2113 (KX) was ligated to the 5′-ends of serial deletion mutants of the 5′-flanking region (bold line) at EcoRI (E), PstI (P) and SalI (S) sites and assayed for promoter activity. Precise lengths of the insert in (A) and (B) can be calculated by parenthesized nucleotide numbering. (C) to (E) Identification of the UpRs. Promoter activity was assayed using various deletion mutants of the genomic region from −520 to −56 with (+, filled bar) or without (−, open bar) ligation of KX (oval symbol). Small rectangles in (E) denote UpSp1 and InvSp1 and a mutant UpSp1 with X. Thin lines in (A), (B) and (D) denote regions skipped by deletion.

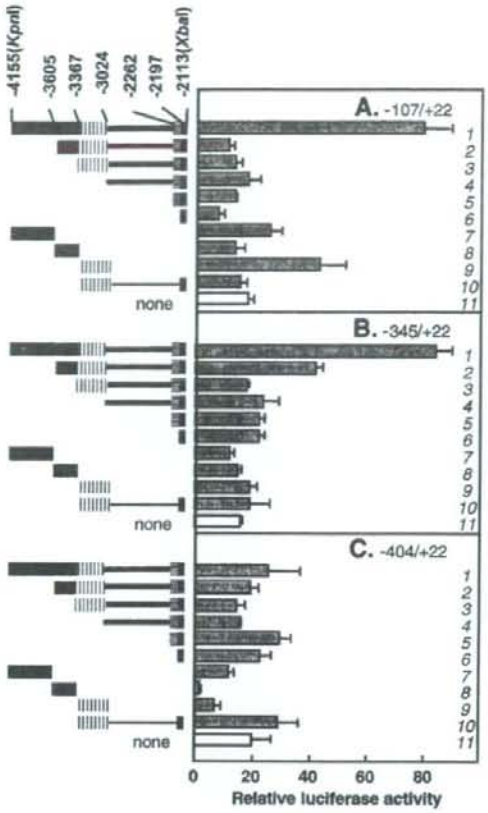

Fig. 5. The potential of segments within KX to change promoter activity with the aid of UpRs. Indicated segments of KX were ligated to 5′-ends of −107/+22 (A), −345/+22 (B), and −404/+22 (C) and assayed for promoter activity in LMH cells. None denotes the recipient DNA alone. Thin lines are the skipped genomic regions. Constructs are verified by the numbering.

the KX-dependent promoter activation was suppressed in the presence of −376/−346 (construct 2 in Fig. 4D) and −137/−108 (construct 3 in Fig. 4E).

3.7. KX-dependent regulator regions

−376/−346 may have suppressor activity, since KX activates the promoter by the removal of −376/−346 (Fig. 4D, constructs 1, 2 and 3). −345/−291 may have an activator whose activity is lost by the cleavage at −319 (Fig. 4D, constructs 3, 4 and 5). The consecutive −376/−346 and −345/−291 regions were thus designated *upstream regulator region 1* for suppression and activation of transcription (UpR1S and UpR1A). Additional suppressor activity was detectable in −137/−108 (Fig. 4E, constructs 3 and 4). −107/−83 by itself slightly increases promoter activity of −82/+22 as −107/+22 (Table 2, Experiment 1 and open bars of constructs 4 and 6 in Fig. 4E). Moreover, −107/−83 appeared to KX-dependently activate the promoter (Fig. 4E, constructs 4 and 6). Therefore, −137/−108 and −107/−83 regions were designated UpR2S and UpR2A. Each UpR appears to abolish the function of an immediately downstream UpR in a hierarchical manner in LMH cells. While −82/+22 was weakly responsible to KX, −56/+22 without UpSp1 was not (Fig. 4E, constructs 6 and 7). −107/+22 with the mutant UpSp1 (M7) was also insufficient to respond to KX (Fig. 4E, constructs 4 and 5). UpSp1 thus appears to be important to the KX-dependent promoter activation.

3.8. Interaction of segments within KX with UpRs

Various fragments derived from KX were ligated to 5′-ends of −107/+22, −345/+22, or −404/+22, which respectively have UpR2A (Fig. 5A), UpR1A, UpR2S and UpR2A (Fig. 5B), and the four UpRs (Fig. 5C). In Fig. 5A, the deletion of −4155/−3605 nullified the promoter activation by UpR2A (constructs 1 and 2). Conversely, −4155/−3605 and −3366/−3024 slightly increased promoter activity by direct ligation to −107/+22 (constructs 7 and 9). A short 3′-end fragment (−2197/−2113) decreased promoter activity of −107/+22 itself (construct 6) and cancelled the promoter activation in −107/+22 by −3366/−3024 (constructs 9 and 10). In Fig. 5B, the deletion of −4155/−3605 from KX (construct 2) decreased the promoter activation to 50% of that by the entire KX (construct 1). Other constructs did not show clear changes in promoter activity, indicating that the three UpRs interact with the promoter in a manner different from that of UpR2A alone. In Fig. 5C, addition of UpR1S to the three UpRs suppressed the promoter (construct 1). Of the fragments from KX, −3604/−3367 strongly and −3366/−3024 weakly suppressed the promoter in the presence of the four UpRs (constructs 8 and 9). Notably, further insertion of −2197/−2113 into the construct 9 abolished this suppression (construct 10). In summary, −4155/−3605 was involved in the promoter activation and −3604/−3367 appeared to suppress it. −3366/−3024 appeared to function in both the promoter activation and its suppression. −2197/−2113 restored promoter activity changed by −3366/−3024 to the basal activity (constructs 9 and 10 in Fig. 5A and C). Conclusively, the four segments within KX participate in the regulation of promoter activity.

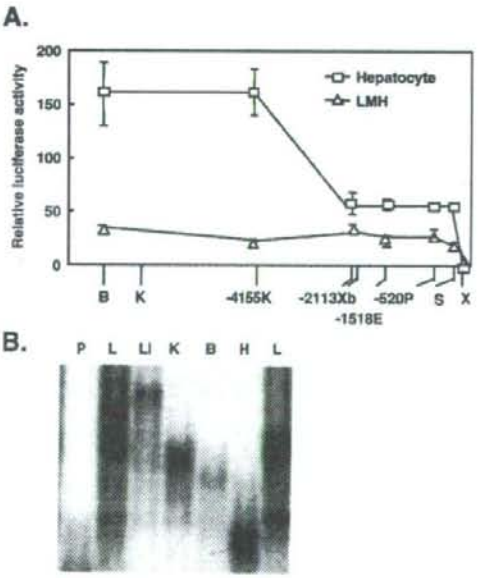

Fig. 6. Cell-type specific functions of KX and UpRs. (A) Recombinant plasmids used in Experiment 1 in Table 2 were assayed for promoter activity in hepatocytes in primary culture (open square) and LMH cells (open triangle). B, K, Xb, E, P, S and X indicate positions used for preparation of serial deletion mutants (see Fig. 1B). (B) EMSA using [^{32}P]-labeled UpR2A (−107/−83) probe and nuclear extracts from LMH cells (lanes L), liver (lane Li), kidney (lane K), brain (lane B) and heart (lane H) from chickens at 4 months of age. Probe alone was loaded onto lane P.

3.9. Cell-type specific regulation of the promoter

To address whether KX similarly functions in hepatocytes and LMH cells, the serial deletion mutants used in Experiment 1 of Table 2 were assayed for luciferase gene expression in hepatocytes in primary culture. Of the six mutants tested, the two constructs with KX (constructs having genomic regions upstream from −2113) increased luciferase activity in hepatocytes to a level 3-fold higher than those expressed by constructs without KX (Fig. 6A). LMH cells, when transfected with identical sets of the plasmids, did not exhibit the KX-dependent change in promoter activity (Experiment 1 in Table 2, and Fig. 6A). Moreover, the constructs without KX yielded higher levels of luciferase in hepatocytes than in LMH cells. These findings support the possibility that UpR1S and UpR2S are at least less active in hepatocytes than in LMH cells probably in a cell-type specific manner.

3.10. Proteins binding to UpR2A

To gain more insight into tissue-specific functions of UpRs, UpR2A (−107/−83) was examined for properties in binding protein (s). EMSA using a [^{32}P]-UpR2A probe revealed that nuclear extracts from the liver, kidney, and brain from chickens at 4 months of age had UpR2A binding proteins that respectively yield a single, clear signal but with mobility intrinsic to each tissue (Fig. 6B, lanes Li, K and B). Nuclear extracts from the heart, which lacks GDC, gave a signal with faster mobility than those revealed for other tissues (Fig. 6B, lane H). LMH cell nuclear extracts yielded signals whose number and mobility differ from those given by the four tissues (Fig. 6B, lanes L). Despite the presence or absence of GDC, the adult chicken tissues likely have UpR2A binding proteins in different populations.

3.11. Putative cis-element in UpR2A

UpR2A was examined by similar procedures for a putative segment to which nuclear proteins can bind. For this purpose, mutant UpR2A competitors were prepared by substitutions of three consecutive nucleotides in every 3-nucleotide interval (Fig. 7A). A wild-type [^{32}P]-UpR2A probe incubated with liver nuclear extracts from chickens at 4 months of age formed a signal similar to that in lane Li in Fig. 6B (Fig. 7B, lane N+, C−). Prior incubation of the nuclear extract with 200-fold molar excess wild-type UpR2A competitor abrogated this signal (lane WT), indicating the binding of protein(s) to particular sequences of UpR2A. This signal was detectable even after prior incubation of the nuclear extract with an M12 mutant competitor (Fig. 7B, lane M12). M14 and M16 competitors also yielded weak signals with a slightly larger mobility than those in lanes N+, C− and M12 (Fig. 7B, lanes M14 and M16). These findings indicate that UpR2A interacts with liver nuclear proteins in a sequence encompassing −104 to −90. In competition with M12, LMH cell nuclear extracts yielded a weak signal with mobility similar to those found in lanes N+, C− and M12 in Fig. 7B (Fig. 7C). Therefore, LMH cells have UpR2A binding proteins similar to those in the liver but in a lesser amount, compared to their hepatic level.

3.12. UpR2A mutants in the KX-dependent promoter activation

We respectively inserted the mutant UpR2A sequences between KX and the promoter region (−82/+22) in pGL3-basic vectors and

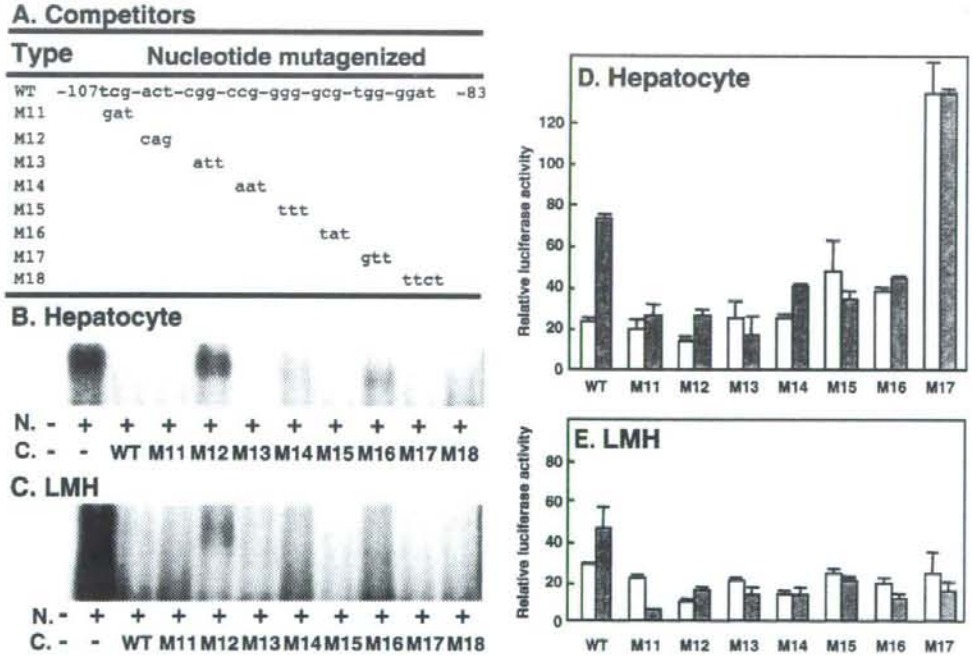

Fig. 7. Binding of nuclear proteins to UpR2A. (A) Structures of wild-type and mutant UpR2A. Three bases mutagenized in mutant UpR2A (M11 to M18) are shown at the corresponding positions along with the wild-type (WT) sequence. (B) and (C) EMSA using [^{32}P]-labeled WT UpR2A probe and wild-type and mutant competitors (WT and M11 to M18 under the panels). Liver nuclear extracts from chickens at 4 months of age and LMH cell nuclear extracts were used in (B) and (C). N and C stand for the nuclear extracts and competitors. (D) and (E) −107/+22 with either WT or M11 to M17 UpR2A were constructed in pGL3-basic vectors and assayed for the promoter activation with (filled bar) or without (open bar) ligation of KX in hepatocytes in (D) and in LMH cells in (E). Control cells were transfected with empty vector.

compared extents of the KX-dependent promoter activation by the mutants with those by wild-type UpR2A in hepatocytes and LMH cells (Fig. 7D and E). In hepatocytes, the wild-type UpR2A construct clearly increases promoter activity (Fig. 7D, filled bar for WT) in a KX-dependent manner to a larger extent than that in LMH cells (Fig. 7E, filled bar for WT). The mutant constructs were defective in the KX-dependency in the promoter activation (Fig. 7D, filled and open bar). Therefore, the binding of nuclear proteins to a segment from −104 to −90 is indispensable to the KX-dependent promoter activation. The M17 construct exhibited extraordinarily high promoter activity, with or without KX, in a manner intrinsic to hepatocytes, although the mechanisms are unclear at present.

3.13. UpR-like sequences around the 5′-end of exon 1 of the human GDC gene

We have shown that regulator regions with the illustrated location (Fig. 8A) are required for chicken GDC gene transcription. The UpR1 and UpR2 sequences do not appear to be highly similar (Fig. 8B). Taking advantage of this feature, we examined whether 5′-flanking and 5′-untranslated regions of the human GDC gene possess regions similar to the chicken UpR1S/UpR1A and UpR2S/UpR2A sequences (Fig. 8C), since chicken and human GDC genes resemble in many respects (Kume et al., 1991; Takayanagi et al., 2000). In this comparison, there were several problems resulting from incorrect understanding of general gene structures by Kure and colleagues (Takayanagi et al., 2000). For example, despite the finding that transcription of the human GDC gene probably begins with the guanine base 163 bases upstream from the adenine base of the translation start codon, the authors confusedly assigned this adenine base to the 5′-end of exon 1 in Table 2 and Fig. 3 (Takayanagi et al., 2000). In this context, we have reported that the human GDC cDNA had a 5′-untranslated sequence comprising 150 bases (Kume et al., 1991). This untranslated sequence is entirely included in the human genomic sequence from −150 to −1 in Fig. 3B by Takayanagi et al. (2000). Therefore, in the present paper, we defined the guanine nucleotide at −163 as a putative 5′-end of exon 1 of the human GDC gene. This definition is extremely important, since human genomic DNA sequences similar to those of UpR1 and UpR2 were found respectively in the 5′-flanking region and in the 5′-untranslated region (Fig. 8C). Notably, the UpR2A segments mutagenized for M12, M14, and M16 preparation appeared to be conserved in the human genomic DNA sequence. The KX segments were not compared with the human DNA sequence, since those are still too long to be used for the comparison.

3.14. Chicken UpR-related sequences in the human genome

The human genome had 19 UpR1- and 7 UpR2-related sequences (Figs. 9 and 10). This suggested and actual comparison of the human and chicken sequences confirmed that the UpR sequences are in part conserved together with binding motifs for transcription factors. The 14 UpR1A-related sequences that resemble the −347/−327 segment (sequence in red) of UpR1A represent the conserved sequence (Fig. 9). This UpR1A region included motifs for YY1 (arrows 1 and 2), δ Factor (a homologue of YY1, arrow 3), repressor of CAR1 expression (arrow 4), T-Ag (arrow 5), RXR and T3R (arrow 6), AML1 (arrow 7), AP-2 (arrow 8) and TCF-4E (arrow 9). These motifs are conserved in most human

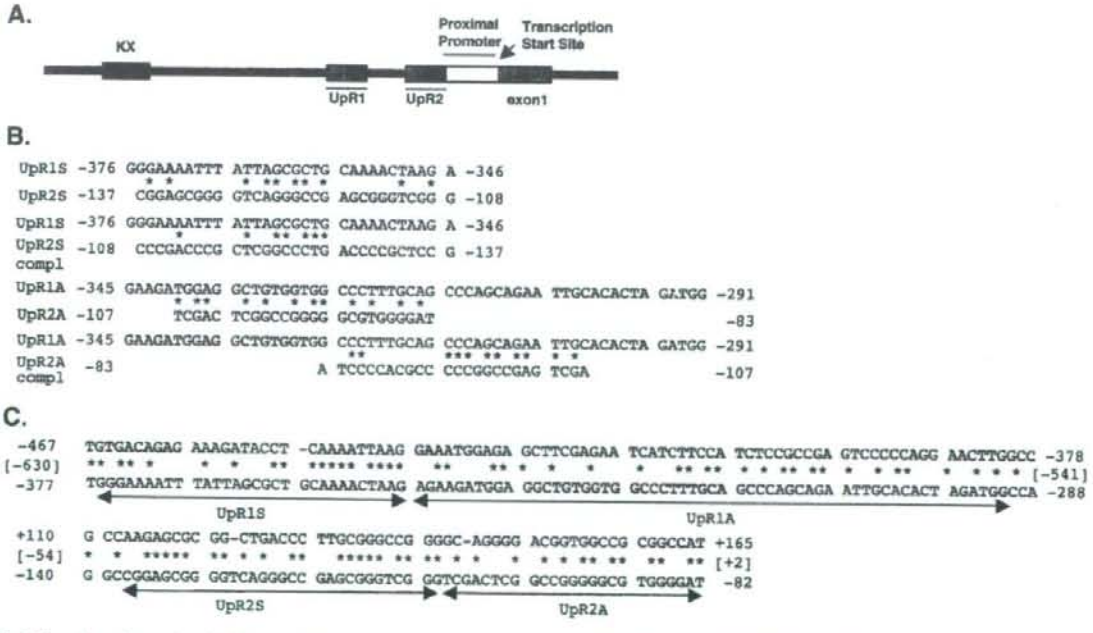

Fig. 8. Genomic regulator regions. (A) Schematic illustration of the chicken KX (red), UpR1S and UpR2S (blue), UpR1A and UpR2A (red), proximal promoter (open bar), and exon 1 (green). (B) Sequence similarity of UpR1S and UpR1A to UpR2S and UpR2A. Identical bases were indicated with asterisks. "Compl" denotes complementary sequence. (C) The human genomic DNA sequences similar to chicken UpR1S/UpR1A and UpR2S/UpR2A. Chicken UpR1S+UpR1A and UpR2S+UpR2A were aligned over 5′-flanking and 5′-untranslated regions of the human GDC gene, respectively. Arrows indicated genomic regions of UpR1S and UpR2S (blue) and UpR1A and UpR2A (red). Based on our conclusion that −163 described by Takayanagi et al. (2000) is the putative transcription start site and +1, the numbering is shown without parenthesis and instead, the numbering by Takayanagi et al. (2000) is parenthesized for human genomic sequences.

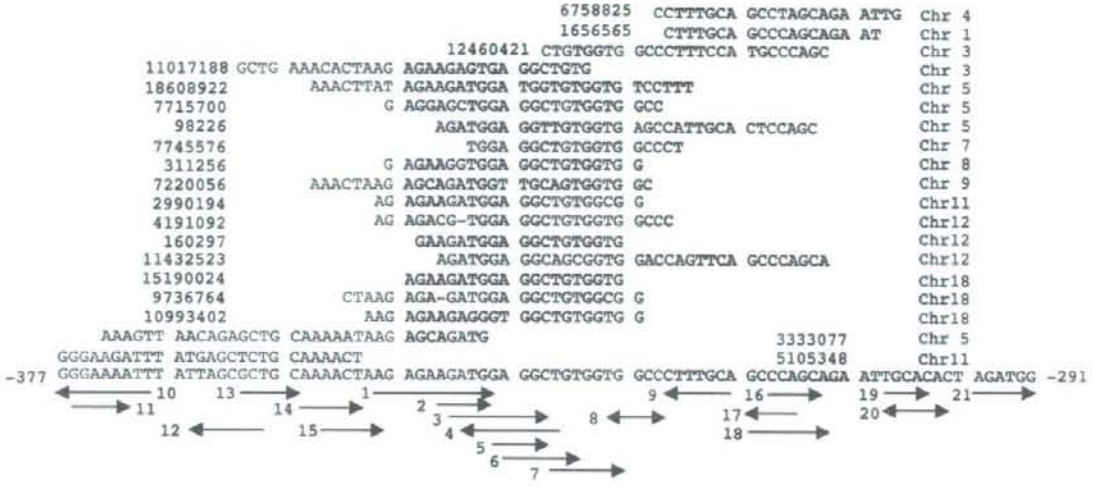

Fig. 9. Human genomic DNA similar to UpR1S+UpR1A. Human genome databases were examined for sequences similar to UpR1S+UpR1A using Blat at UCSC and Blast at NCBI. Chicken UpR1 sequence were examined for transcription factor binding motifs by Patch at Gene-regulation. com (http://www.gene-regulation.com/). Arrows indicate positions of predicted motifs. In the bottom row, UpR1S and UpR1A are shown in gray and black. The region indicated in red is the region most prevalent in the human genome. Human DNA sequences similar to part of UpR1 sequence were shown together with chromosome number and nucleotide position at one end.

DNA regions. UpR1S shown in gray had motifs for C/EBP isoforms (arrow 10), ICGF-3 and NFAT isoforms (arrow 11), E2F isoforms (arrow 12), CTCF (arrow 13), AR (arrow 14) and HNF-4α (arrow 15). The 3′ half of UpR1A had motifs for LBP-1 (arrow 16), T-Ag (arrow 17), AP-2 (arrow 18), Sp1 (arrow 19), GR and MTF-1 (arrow 20), and YY1 (arrow 21). Fig. 10 indicates that most human sequences conserved correspond to UpR2S sequence. In UpR2S, motifs for YY1 (arrow 1), GAGA factor (arrows 2 and 6), LMC (arrow 3), FXR and RXR (arrow 4), AP-1, T3R, COUP and RAR (arrow 5 and 7) are present. In UpR2A, those for ARP-1 (arrow 8), PAI-2 (arrow 9), Glob-B (arrow 10), AP-2 and HNF-3 (arrow 11), C-ACT (arrow 12), T-Ag (arrow 13), AhR and Arnt (arrow 14) and AP-2, MBP-1, and NFκB (arrow 15) are present. Of 7 human chromosomes, chromosome 15 had a sequence similar (76%) to a segment from −136 to −84 of UpR2 with 1 gap together with motifs shown with arrows 1 to 3, 6 and 8. This begins 70 bases upstream from the transcription start site of the human cellular retinoic acid binding protein gene. Chromosome 19 DNA had −140/−114 of UpR2S as the +40/+66 region of the human intron-less Jun D proto-oncogene. These regions might function in the regulation of transcription and translation. A motif (−104/−97, arrow 10) for Glob-B (a transactivator of β-globin locus control region) (Walters et al., 1991), which is an LSF/Grainyhead transcription factor family member (Venkatesan et al., 2003), notably encompasses the M12 region (−104/−102). Another family member might bind to this motif in hepatocytes. Motifs for YY1 and CTCF, which are known as a silencer or an insulator (Baniahmad et al., 1990; Shirra and Hansen, 1998; Fourel et al., 2002; West et al., 2002; Kim et al., 2003), are present together with that for δ factor (a homolog of YY1) in a UpR1S/UpR1A boundary region. YY1 sites are also present in the 3′-end of UpR1A and in UpR2S, suggesting that these factors function in the suppression of the GDC gene promoter.

4. Discussion

The present study has clarified for the first time several structural and functional characteristics involved in the regulation of vertebrate GDC gene transcription. The chicken GDC gene comprises 25 exons with the entire sequence of 3572 bases in the region between 202,503 and 240,569 on the chromosome Z minus strand (accession number: AC202790) and encodes the active site lysine residue in exon 19. −82/+22, which has binding motifs similar to those for the known Sp1, NF-Y and CP2, is absolutely required for promoter activity. All the *cis*-elements bind nuclear proteins. UpSp1, InvSp1 and the downstream CP2 motifs are indispensable for promoter activity. Thus, we assigned −82/+22 to the chicken GDC gene proximal promoter.

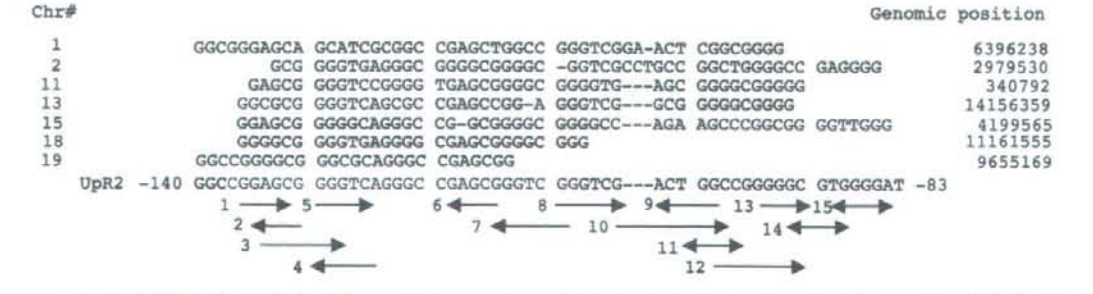

Fig. 10. Human genomic DNA similar to UpR2S+UpR2A. Human genomic sequences were selected and analyzed by the procedures similar to those used in Fig. 9. UpR2S and UpR2A are shown in gray and black, respectively.

Promoter assays in LMH cells and hepatocytes have clarified that a 5′-flanking region from −4155 to −83 encompasses KX, UpR1S, UpR1A, UpR2S and UpR2A regions that may change promoter activity. −4155/−3605, −3604/−3367, −3366/−3024 and −2197/−2113 within KX appeared to have the potential to interact with different UpR counterparts, since these segments in KX activate, suppress or restore promoter activity in various types of recombinant constructs in which KX coexists with one to four UpRs and the proximal promoter (Fig. 5). In the promoter, UpSp1 (−71 to −62), which is the most upstream element, is 12 bases downstream from UpR2A. A −107/+22 construct with a mutagenized UpSp1 (M7 in Table 2 and construct 5 in Fig. 4E) largely lost both the promoter activity and the potential to respond to KX and UpR2A in the promoter activation. The native genomic organization of the four regions in KX, the four UpRs and the elements in the proximal promoter is thought to be prerequisite for their cooperation in chicken GDC gene transcription regulation.

Taking general mechanisms of transcription regulation into account, it is likely that these genomic regions recruit proteins to accomplish the regulation. Actually, in UpR2A, the −104/−102 segment is indispensable to bind liver nuclear protein(s). The Glob-B binding motif, GACTGGC (Walters et al., 1991), encompasses this segment. Proteins recognize the motif might play a principal role in the promoter activation. Low sequence similarity of the four UpRs suggested different categories of the functions of the UpRs. Actually, this was emphasized by the finding that transcription factors predicted likely assign UpR1S and UpR2S to suppressor or insulator and UpR1A and UpR2A to enhancer. Molecular characterization of the binding proteins would clarify roles of the four UpRs in GDC gene transcription.

On the genomic DNA stretch, UpR2S and UpR2A can be localized on an identical nucleosome together with the proximal promoter. UpR1S and UpR1A may be located on the adjacent nucleosome, whereas the segments in KX are estimated to be 15 to 30 nucleosomes distant from the 5′-end of UpR2A. Therefore, mechanisms by which particular regions in KX are placed in proximity to the promoter are thought to be most important in the regulation of GDC gene transcription. Looping of the nucleosomal stretch is an attractive mechanism by which KX regulates promoter activity with the aid of the four UpRs. Histone modification by acetylation (Pazin and Kadonaga, 1997; Struhl, 1998; Bulger, 2005), methylation (Tachibana et al., 2002), phosphorylation (Pantazis et al., 1984), ADP-ribosylation (Kim et al., 2005), and sumoylation (Nathan et al., 2003) might mediate chromatin remodeling to recruit proteins that bind to KX and the UpRs. Covalent DNA modification such as DNA methylation is a critical mechanism for chromatin remodeling (Klose and Bird, 2006).

The chicken GDC gene promoter is GC-rich as described in Results. In mammals, Weber et al. (2007) classified GC-rich promoter into three categories: high-, low- and intermediate-CpG promoters (HCP, LCP and ICP) by measuring G, C and CpG contents. According to their equation, the chicken GDC gene promoter with 0.96 of the ratio belongs to HCP (the ratio>0.75). Unlike LCP, hypermethylation of which decreases transcription activity, HCP was mostly hypomethylated and active in transcription in mammalian somatic cells. In this context, chromosomes Z and W determine the sexuality as Z/Z for male and Z/W for female. In humans, DNA methylation is involved in embryonic development, genomic imprinting, and X-chromosome inactivation. If chicken cells mimic these events, the GDC gene promoter might be a target for such regulation during embryogenesis. In the combination of the various types of reactions for chromatin remodeling and the functions of the four UpRs, chicken cells can determine GDC levels intrinsic to individual cells.

In a physiological aspect, GDC expression plays a key role in determining tissue-specific distribution of glycine cleavage activity. Previously, we showed that different GDC levels in different tissues are predominantly determined at the level of GDC gene transcription (Kure et al., 1991a). In the present study, we found several lines of evidence related to cell-type specific expression of GDC: 1) Chicken GDC gene promoter (−82/+22) may change transcription activity with the aid of KX and UpRs (Fig. 4A to E). 2) GDC gene promoter activity exhibited by the entire 5′-flanking sequence changes in response to types of recipient cells such as hepatocytes and LMH cells probably due to differences in use of UpR1S and UpR2S (Fig. 6A). 3) A construct (KX/UpR2A/promoter) prepared by direct ligation of KX to −107/+22 exhibited promoter activity to different extents in hepatocytes and LMH cells (columns for WT in Fig. 7D and E). 4) UpR2A binding proteins are present in various tissues in different populations (Fig. 6B). These functional properties support the possibility that the KX-dependent and UpR-mediated regulation of GDC gene transcription is a principal mechanism of GDC expression intrinsic to particular types of cells. Accordingly, together with the mechanisms for chromatin remodeling, KX and the four UpRs and the promoter binding proteins are physiologically relevant to determine glycine catabolism in various chicken tissues at different ages.

The 5′-flanking region and the 5′-untranslated region of the human GDC gene had sequences similar to UpR1S/UpR1A and UpR2S/UpR2A, respectively (Fig. 8). It is likely that these regions are human versions of UpR1 and UpR2, although the human GDC gene promoter has never been characterized. Of the genes for the three intrinsic components of the glycine cleavage system, the GDC gene is most prevalently responsible for defective glycine cleavage activity in patients with nonketotic hyperglycinemia (Kume et al., 1988; Sakakibara et al., 1990; Kure et al., 1991a,b, 2006; Kanno et al., 2007). The deletion at 5′-regions of this gene has been assigned as a major cause of this disease (Sakakibara et al., 1990; Kanno et al., 2007). The present study suggested that the 5′-region of the chicken GDC gene by nature is likely flexible and mobile to accomplish the KX-dependent and UpR-mediated regulation. If the putative UpR1 and UpR2 segments similarly function in human cells, then the exonic sequence similar to UpR2S/UpR2A might confer the human GDC gene a complicated conformation in the course of the mutual conversion of the activated, suppressed and silenced conformations of the promoter at the initial stage of human reproduction including germ cell production. These physiological mechanisms might fortuitously be a cue for the pathological deletions of the human GDC gene. Molecular characterization of the KX-dependent and UpR-mediated regulation of the GDC gene promoter would help better understanding of the physiological and pathological implications of chicken and human GDC gene transcription. In future study, the UpR2A binding protein(s) that must interact with proteins binding to upstream and downstream elements should be initially identified to delineate the problem of interest.

Acknowledgement

This work was supported in part by a Grant-in-Aid (14370052) from the Ministry of Education, Culture, Sports, Science and Technology, Japan.

References

Baniahmad, A., Steiner, C., Kohne, A.C., Renkawitz, R., 1990. Modular structure of a chicken lysozyme silencer: involvement of an unusual thyroid hormone receptor binding site. Cell 61, 505–514.

Breathnach, R., Chambon, P., 1981. Organization and expression of eukaryotic split genes coding for proteins. Annu. Rev. Biochem. 50, 349–383.

Bulger, M., 2005. Hyperacetylated chromatin domains: lessons from heterochromatin. J. Biol. Chem. 280, 21689–21692.

Calzone, F.J., Britten, R.J., Davidson, E.H., 1987. Mapping of gene transcripts by nuclease protection assays and cDNA primer extension. Methods Enzymol. 152, 611–632.

Chodosh, L.A., Baldwin, A.S., Carthew, R.W., Sharp, P.A., 1988. Human CCAAT-binding proteins have heterologous subunits. Cell 53, 11–24.

Chomczynski, P., Sacchi, N., 1987. Single-step method of RNA isolation by acid guanidinium thiocyanate-phenol-chloroform extraction. Analyt. Biochem. 162, 156–159.

Corden, J., Wasylyk, B., Buchwalder, A., Sassone-Corsi, P., Kedinger, C., Chambon, P., 1980. Promoter sequences of eukaryotic protein-coding genes. Science 209, 1406–1414.

Dignam, J.D., Lebovitz, R.M., Roeder, R.G., 1983. Accurate transcription initiation by RNA polymerase II in a soluble extract from isolated mammalian nuclei. Nucleic Acids Res. 11, 1475–1489.
Dynan, W.S., Tjian, R., 1983. The promoter-specific transcription factor Sp1 binds to upstream sequences in the SV40 early promoter. Cell 35, 79–87.
Fourel, G., Lebrun, E., Gilson, E., 2002. Protosilencers as building blocks for heterochromatin. Bioessays 24, 828–835.
Gustincich, S., et al., 2006. The complexity of the mammalian transcriptome. J. Physiol. 575, 321–332.
Henikoff, S., 1984. Unidirectional digestion with exonuclease III creates targeted breakpoints for DNA sequencing. Gene 28, 351–359.
Hennighausen, L., Lubon, H., 1987. Interaction of protein with DNA in vitro. Methods Enzymol. 152, 721–735.
Hibino, Y., et al., 2006. Molecular properties and intracellular localization of rat nuclear scaffold protein P130. Biochim. Biophys. Acta 1759, 195–207.
Hiraga, K., Kikuchi, G., 1980a. The mitochondrial glycine cleavage system: purification and properties of glycine decarboxylase from chicken liver mitochondria. J. Biol. Chem. 255, 11664–11670.
Hiraga, K., Kikuchi, G., 1980b. The mitochondrial glycine cleavage system: functional association of glycine decarboxylase and aminomethyl carrier protein. J. Biol. Chem. 255, 11671–11676.
Hong, S.-P., Piper, M.D., Sinclair, D.A., Dawes, I.W., 1999. Control of expression of one-carbon metabolism genes of *Saccharomyces cerevisiae* is mediated by a tetrahydrofolate-responsive protein binding to a glycine regulatory region including a core 5′-CTTCTT-3′ motif. J. Biol. Chem. 274, 10523–10532.
Isobe, M., Koyata, H., Sakakibara, T., Momoi-Isobe, K., Hiraga, K., 1994. Assignment of the true and processed genes for human glycine decarboxylase to 9p23–24 and 4q12. Biochem. Biophys. Res. Commun. 203, 1483–1487.
Kanno, J., et al., 2007. Genomic deletion within GLDC is a major cause of non-ketotic hyperglycinemia. J. Med. Genet. 44, e69.
Kawaguchi, T., Nomura, K., Hirayama, Y., Kitagawa, T., 1987. Establishment and characterization of a chicken hepatocellular carcinoma cell line, LMH. Cancer Res. 47, 4460–4464.
Kikuchi, G., 1973. The glycine cleavage system: composition, reaction mechanism, and physiological significance. Mol. Cell. Biochem. 1, 169–187.
Kikuchi, G., Hiraga, K., 1982. The mitochondrial glycine cleavage system: unique features of the glycine decarboxylation. Mol. Cell. Biochem. 45, 137–149.
Kikuchi, G., Motokawa, Y., Yoshida, T., Hiraga, K., 2008. The glycine cleavage system: reaction mechanism, physiological significance, nonketotic hyperglycinemia. Proc. Japan Acad. Ser. B. 84, 246–262.
Kim, J., Kollhoff, A., Bergmann, A., Stubbs, L., 2003. Methylation-sensitive binding of transcription factor YY1 to an insulator sequence within the paternally expressed imprinted gene, Peg3. Hum. Mol. Genet. 12, 233–245.
Kim, M.Y., Zhang, T., Kraus, W.L., 2005. Poly(ADP-ribosyl)ation by PARP-1: 'PAR-laying' NAD+ into a nuclear signal. Genes Dev. 19, 1951–1967.
Klose, R.J., Bird, A.P., 2006. Genomic DNA methylation: the mark and its mediators. Trends Biochem. Sci. 31, 89–97.
Kume, A., Kure, S., Tada, K., Hiraga, K., 1988. The impaired expression of glycine decarboxylase in patients with hyperglycinemias. Biochem. Biophys. Res. Commun. 154, 292–297.
Kume, A., Koyata, H., Sakakibara, T., Ishiguro, Y., Kure, S., Hiraga, K., 1991. The glycine cleavage system: molecular cloning of the chicken and human glycine decarboxylase cDNAs and some characteristics involved in the deduced protein structures. J. Biol. Chem. 266, 3323–3329.
Kure, S., Koyata, H., Kume, A., Ishiguro, Y., Hiraga, K., 1991a. The glycine cleavage system: the coupled expression of the glycine decarboxylase gene and the H-protein gene in the chicken. J. Biol. Chem. 266, 3330–3334.
Kure, S., Narisawa, K., Tada, K., 1991b. Structural and expression analyses of normal and mutant mRNA encoding glycine decarboxylase: three-base deletion in mRNA causes nonketotic hyperglycinemia. Biochem. Biophys. Res. Commun. 174, 1176–1182.
Kure, S., et al., 2006. Comprehensive mutation analysis of GLDC, AMT, and GCSH in nonketotic hyperglycinemia. Hum. Mutat. 27, 343–352.
Lim, C.L., Fang, L., Swendeman, S.L., Sheffery, M., 1993. Characterization of the molecularly cloned murine α-globin transcription factor CP2. J. Biol. Chem. 268, 18008–18017.
Maniatis, T., Goodbourn, S., Fischer, J.A., 1987. Regulation of inducible and tissue-specific gene expression. Science 236, 1237–1245.
Mantovani, R., et al., 1992. Monoclonal antibodies to NF-Y define its function in MHC class II and albumin gene transcription. EMBO J. 11, 3315–3322.
Matsui, C., Koyata, H., Hiraga, K., 1993. The development-associated increase in the hepatic levels of the intrinsic components of the chicken glycine cleavage system. Arch. Biochem. Biophys. 300, 69–74.
Murata, T., Nitta, M., Yasuda, K., 1998. Transcription factor CP2 is essential for lens-specific expression of the chicken αA-crystallin gene. Genes Cells 3, 443–457.
Nakai, T., Nakagawa, N., Maoka, N., Masui, R., Kuramitsu, S., Kamiya, N., 2005. Structure of P-protein of the glycine cleavage system: implications for nonketotic hyperglycinemia. EMBO J. 24, 1523–1536.
Nathan, D., Sterner, D.E., Berger, S.L., 2003. Histone modifications: now summoning sumoylation. Proc. Natl. Acad. Sci. U.S.A. 100, 13118–13120.
Nyhan, W.L., 1989. Nonketotic hyperglycinemia. In: Scriver, C.R., Beaudet, M.D., Sly, W.S., Valle, D. (Eds.), The Metabolic Basis of Inherited Disease, 6th Ed. McGraw-Hill Information Services Co., New York, pp. 743–753.
Okamura-Ikeda, K., Ohmura, Y., Fujiwara, K., Motokawa, Y., 1993. Cloning and nucleotide sequence of the gcv operon encoding the *Escherichia coli* glycine-cleavage system. Eur. J. Biochem. 216, 539–548.
Pantazis, P., West, M.H., Bonner, W.M., 1984. Phosphorylation of histones in cells treated with hypertonic and acidic media. Mol. Cell. Biol. 4, 1186–1188.
Pazin, M.J., Kadonaga, J.T., 1997. What's up and down with histone deacetylation and transcription? Cell 89, 325–328.
Sakakibara, T., et al., 1990. One of the two genomic copies of the glycine decarboxylase cDNA has been deleted at a 5′ region in a patient with nonketotic hyperglycinemia. Biochem. Biophys. Res. Commun. 173, 801–806.
Seglen, P.O., 1976. Preparation of isolated rat liver cells. Methods Cell Biol. 13, 29–34.
Shirra, M.K., Hansen, U., 1998. LSF and NTF-1 share a conserved DNA recognition motif yet require different oligomerization states to form a stable protein–DNA complex. J. Biol. Chem. 273, 19260–19268.
Sinclair, D.A., Hong, S.-P., Dawes, I.W., 1996. Specific induction by glycine of the gene for the P-subunit of glycine decarboxylase from *Saccharomyces cerevisiae*. Mol. Microbiol. 19, 611–623.
Smale, S.T., Baltimore, D., 1989. The "initiator" as a transcription control element. Cell 57, 103–113.
Struhl, K., 1998. Histone acetylation and transcriptional regulatory mechanisms. Genes Dev. 12, 599–606.
Tachibana, M., et al., 2002. G9a histone methyltransferase plays a dominant role in euchromatic histone H3 lysine 9 methylation and is essential for early embryogenesis. Genes Dev. 16, 1779–1791.
Takayanagi, M., et al., 2000. Human glycine decarboxylase gene (GLDC) and its highly conserved processed pseudogene (psiGLDC): their structure and expression, and the identification of a large deletion in a family with nonketotic hyperglycinemia. Human. Genet. 106, 298–305.
van Huijsduijnen, R.H., Li, X.Y., Black, D., Matthes, H., Benoist, C., Mathis, D., 1990. Co-evolution from yeast to mouse: cDNA cloning of the two NF-Y (CP-1/CBF) subunits. EMBO J. 9, 3119–3127.
Venkatesan, K., MacManus, H.R., Mello, C.C., Smith, T.F., Hansen, U., 2003. Functional conservation between members of an ancient duplicated transcription factor family, LSF/Grainyhead. Nucleic Acids Res. 31, 4304–4316.
Walters, M., Kim, C., Gelinas, R., 1991. Characterization of a DNA binding activity in DNAse I hypersensitive site 4 of the human globin locus control region. Nucleic Acids Res. 19, 5385–5393.
Weber, M., et al., 2007. Distribution, silencing potential and evolutionary impact of promoter DNA methylation in the human genome. Nat. Genet. 39, 457–466.
West, A.G., Gaszner, M., Felsenfeld, G., 2002. Insulators: many functions, many mechanisms. Genes Dev. 16, 271–288.
Wilson, R.L., Stauffer, G.V., 1994. DNA sequence and characterization of GcvA, a LysR family regulatory protein for the *Escherichia coli* glycine cleavage enzyme system. J. Bacteriol. 176, 2862–2868.
Wilson, R.L., Steiert, P.S., Stauffer, G.V., 1993. Positive regulation of the *Escherichia coli* glycine cleavage enzyme system. J. Bacteriol. 175, 902–904.
Yamamoto, M., Koyata, H., Matsui, C., Hiraga, K., 1991. The glycine cleavage system: occurrence of two types of chicken H-protein mRNAs presumably formed by the alternative use of the polyadenylation consensus sequences in a single exon. J. Biol. Chem. 266, 3317–3322.

Gene Therapy (2008), 1–9

www.nature.com/gt

ORIGINAL ARTICLE

Systemic delivery of IL-10 by an AAV vector prevents vascular remodeling and end-organ damage in stroke-prone spontaneously hypertensive rat

T Nomoto[1,2], T Okada[1,3], K Shimazaki[4], T Yoshioka[1], M Nonaka-Sarukawa[1], T Ito[1], K Takeuchi[5], K-i Katsura[2], H Mizukami[1], A Kume[1], S Ookawara[5], U Ikeda[6], Y Katayama[2] and K Ozawa[1]

[1]*Division of Genetic Therapeutics, Center for Molecular Medicine, Jichi Medical University, Tochigi, Japan;* [2]*Second Department of Internal Medicine, Nippon Medical School, Tokyo, Japan;* [3]*Department of Molecular Therapy, National Institute of Neuroscience, National Center of Neurology and Psychiatry, Tokyo, Japan;* [4]*Department of Physiology, Jichi Medical University, Tochigi, Japan;* [5]*Department of Anatomy, Jichi Medical University, Tochigi, Japan and* [6]*Department of Cardiovascular Medicine, Shinshu University Graduate School of Medicine, Nagano, Japan*

Interleukin-10 (IL-10) ameliorates various T-helper type 1 cell-mediated chronic inflammatory diseases. Although the therapeutic benefits of IL-10 include antiatherosclerotic effects, pathophysiological effects of IL-10 on vascular remodeling in hypertension have not yet been elucidated. These studies were designed to determine whether sustained IL-10 expression, mediated by an adeno-associated virus (AAV) vector, prevents vascular remodeling and target-organ damage in the stroke-prone spontaneously hypertensive rat (SHR-SP)—an animal model of malignant hypertension. A single intramuscular injection of an AAV1 vector encoding rat IL-10 introduced long-term IL-10 expression. These IL-10-transduced rats had decreased stroke episodes and proteinuria, resulting in improved survival. Histological examination revealed a reduced level of deleterious vascular remodeling of resistance vessels in the brain and kidney of these rats. Immunohistochemical analysis indicated that IL-10 inhibited the enhanced renal transforming growth factor-β expression and perivascular infiltration of monocytes/macrophages and nuclear factor-κB-positive cells normally observed in the SHR-SP. Four weeks after IL-10 vector injection, systolic blood pressure significantly decreased and this effect persisted for several months. Overall, AAV vector-mediated systemic IL-10 expression prevented vascular remodeling and inflammatory lesions of target organs in the SHR-SP. This approach provides significant insights into the prevention strategy of disease onset with unknown genetic predisposition or intractable polygenic disorders.

Gene Therapy advance online publication, 25 September 2008; doi:10.1038/gt.2008.151

Keywords: *IL-10; AAV vector; vascular remodeling; stroke; hypertension; SHR-SP*

Introduction

Interleukin-10 (IL-10), a pleiotropic cytokine produced by type-2 helper T (Th) cells, regulates inflammatory reactions. Specifically, it inhibits macrophage activation, T-cell proliferation and proinflammatory cytokine production, including the release of interferon (IFN)-γ, IL-2 and tumor necrosis factor-β from Th type 1 (Th1) cells.[1,2] The importance of inflammation in the pathogenesis of atherosclerosis has been increasingly acknowledged.[3] Recent studies have shown that IL-10 decreases atherosclerotic lesions in the large vessels through an anti-inflammatory mechanism.[4–6] We also reported that in ApoE-deficient mice, a single intramuscular adeno-associated virus (AAV) vector injection resulted in sustained IL-10 expression for over 6 months and improved atherosclerosis.[7]

Correspondence: Dr K Ozawa or Dr T Okada, Division of Genetic Therapeutics, Center for Molecular Medicine, Jichi Medical University, 3311-1 Yakushiji, Shimotsuke, Tochigi 329-0498, Japan.
E-mail: kozawa@jichi.ac.jp or t-okada@ncnp.go.jp
Received 22 May 2008; revised 31 July 2008; accepted 1 August 2008

Several evidences suggest that IL-10 regulates endothelial NOS, endothelin-1 and heme oxygenase-1 that substantially associate with blood pressure and vascular remodeling of resistance artery in a genetic model of hypertension. Although the overall contribution of inflammation to vascular damage in patients with hypertension remains to be clarified, several forms of experimental hypertension have been used to demonstrate monocyte/macrophage infiltration into the vessels of target organs, such as the brain and kidney.[8,9] Circulating monocytes are activated in hypertensive patients,[10] and mechanically stretched human monocytic cells induce expression of inflammation-related genes.[11] The spontaneously hypertensive rat (SHR) and its stroke-prone substrain, the stroke-prone spontaneously hypertensive rat (SHR-SP), are well-characterized models of genetic hypertension that mimic human essential hypertension.[12] Recent evidence indicates that an inflammatory reaction may underlie the pathogenesis of arteriolosclerosis in the SHR.[13,14] As a consequence, the role of inflammation in vascular remodeling associated with hypertension-induced organ damage is being researched avidly. However, the role of IL-10 in regulating